

METALS RECOVERY FROM WASTE SOLUTION
USING BIOADSORBENTS DERIVED FROM
BIOMASS WASTES

OMIT MEHFUZ



**METALS RECOVERY FROM WASTE SOLUTION USING BIOADSORBENTS
DERIVED FROM BIOMASS WASTES**

By

© OMIT MEHFUZ

A Thesis submitted to the School of Graduate Studies
in partial fulfillment of the requirements for the degree of

MASTER OF ENGINEERING

Faculty of Engineering and Applied Science
Memorial University of Newfoundland

JULY, 2012

St. John's, Newfoundland, Canada.

ABSTRACT

This research work was divided into 2 parts as mentioned below

PART 1: REMOVALS OF HEAVY METALS FROM ACID MINE DRAINAGE (AMD) USING BIOADSORBENTS FROM ORANGE WASTE

Acid mine drainage (AMD) is worldwide environmental problem concerning both active and closed mining operation. AMD results from microbial oxidation of pyrite in presence of water and air, affording an acidic solution that contains toxic metal ions such as lead(Pb), copper(Cu), zinc(Zn). It causes environmental pollution that affects many countries having historic or current mining industries. In the other hand Saponified orange juice residue(SOJR) was found to be effective for the complete and selective removal of Pb(II), Cu(II) and Zn(II). At the present study, the use of SOJR was investigated as effective, environmentally friendly and low cost bioadsorbent to clean up AMD generated at the Lucky Strike deposit of lead-copper-zinc-gold-silver mine in central Newfoundland, Canada. In this research pH, sorbent dose and initial concentration were found to be most effective for the removal of the contaminants. The effective pH range was found 3 to 5. The selectivity order for metal ion uptake by the adsorbent was Pb(II)>Cu(II)>Zn(II). The maximum loading capacities for Pb(II), Cu(II) and Zn(II) were found as 0.25, 0.43 and 0.134 molkg⁻¹, respectively. The experimental results suggest that SOJR is quite effective for removing heavy metal ions from the acidic solution or mine site polluted water. Based on these results, it can be concluded that, the use of SOJR has the potential to provide effective methods for the treatment of AMD.

PART 2: RECOVERY OF GOLD FROM SYNTHETIC SOLUTION USING CELLULOSE BASE BIOADSORBENTS FROM PAPER AND CLOTH

Realizing a need to develop environmentally benign metallurgical technology for precious metals, I prepared two types of cellulose based adsorption gels, derived from biomass waste such as cloth and paper. Both of these adsorption gels were found to be effective for the adsorption of Gold(Au), from weak to strong hydrochloric acid media. In contrast, other precious metal like Platinum(Pt), and Palladium(Pd) and base metals such as, lead(Pb), copper(Cu), iron(Fe), nickel(Ni), and Zinc(Zn) were almost not adsorbed on either gel. From the adsorption isotherms, the maximum adsorption capacity of the cellulose based adsorbents for Au(III) was estimated to be 1.98 mol kg^{-1} (388 g kg^{-1}) and 1 mol kg^{-1} (196 g kg^{-1}) for cloth and paper, respectively. Gold was adsorbed on the gels according to the Langmuir adsorption model, and the highest maximum adsorption capacity of those gels were observed for Au(III). To improve reaction kinetics, various solid liquid ratios were examined and 90% adsorption was found in the first 15 min for solid liquid ratio higher than or equal to five. Innovative use of these novel adsorption gels can fulfill the need of cost effective and environmentally friendly mean for the recovery of valuable metals.

ACKNOWLEDGEMENTS

The work reported in this paper has been carried out at the Hydrometallurgy Lab, at the Bruneau Centre for Research and Innovation (former INCO Innovation Centre (IIC)), Memorial University of Newfoundland, during the period 2010-2012.

I would like to acknowledge my deep indebtedness to my research supervisor Dr. Shafiq Alam for his continuous guidance, constructive suggestions, sincere co-operation, and constant encouragement. I am also grateful to him for providing me with the opportunity to get the job done in a relatively independent manner.

My special acknowledgement goes to my wife and my son, Tanjila and Ovro, who sacrificed and deprived themselves from my companionship and recreation for the successful completion of my program.

Sincere thanks and gratitude are extended to professors in the Faculty of Engineering and Applied Science for courses they offered and to my fellow graduate students for friendship and pleasant memories we shared in the last two years. Finally I am profoundly grateful to my parents and rest of my family members for their love, support and encouragement.

TABLE OF CONTENTS

ABSTRACT	iii
ACKNOWLEDGEMENTS	iv
TABLE OF CONTENTS	v
LIST OF TABLES	xi
LIST OF FIGURES	xiii
LIST OF SYMBOLS, NOMENCLATURE OR ABBREVIATIONS	xv
LIST OF APPENDIXES	xxi
PART 1 Removals of Heavy Metals from Acid Mine Drainage (AMD)	1-65
using Bioadsorbent from Orange Waste	
Chapter 1	2
1 Introduction	2
1.1 Background	2
1.2 Objective of the Research Work	6
1.3 Organization of the Part of Thesis	7
Chapter 2	8
2 Literature Review	8
2.1 Mining and Acid Mine Drainage	8
2.1.1 Mining	8
2.1.2 Acid Mine Drainage	9
2.1.2.1 Heavy Metal in Acid Mine Drainage	11
2.1.2.2 Pollution by Lead	11

2.1.2.3 Pollution by Copper	13
2.2 Removal of Heavy Metal from Acid Mine Drainage	14
2.2.1 Adsorption	15
2.2.2 Adsorbents	16
2.3 Bioadsorption and Bioadsorbents	16
2.4 Orange Peel	17
2.5 Chemical Analysis Device	19
2.5.1 Chemical Analysis by ICP-OES	19
2.5.1.1 Mechanism	20
2.5.2 Chemical Analysis by FT-IR	22
2.5.3 Chemical Analysis by XRD	23
2.5.3.1 Theoretical Considerations	24
2.5.4 Chemical Analysis by SEM	26
2.5.4.1 Scanning process and image formation	27
2.5.4.2 Magnification	28
2.5.4.3 Sample Preparation	28
Chapter 3	30
3 Materials and Methods	30
3.1 Preparation of Metal Ion Solutions/Chemicals and Analysis	30
3.2 Preparations of the Adsorption Gel from Orange Juice Residue	31
3.3 Analysis	32
3.4 Batch Wise Adsorption Tests	32
3.5 Kinetic Studies	34

3.6 Isotherm and Kinetic Models	34
3.7 XRD Analysis	36
3.8 FT-IR Analysis	36
3.9 Scanning Electron Microscope (SEM) Analysis	37
Chapter 4	38
4 Results and Discussions	38
4.1 Characterization of the Adsorbent	38
4.2 Adsorptive Removal of Metal Ions	39
4.3 Effect of Solid/Liquid Ratio on Metal Adsorption	41
4.4 Influence of pH for the Metal Adsorption	44
4.5 Adsorption Isotherms	45
4.6 Kinetic Studies	51
4.7 Proposed Mechanism of Metal Adsorption	52
4.8 XRD Analysis Result	53
4.9 FT-IR Analysis Result	54
4.10 Scanning Electron Microscope (SEM) Analysis	57
4.11 Research Findings	61
Chapter 5	63
5 Conclusion and Recommendation	63
5.1 Conclusion	63
5.2 Recommendation for Future Work	64

PART 2 Recovery of gold from synthetic solution using cellulose base 65-125**bioadsorbent from paper and cloth**

Chapter 6	66
6 Introduction	66
6.1 Background	66
6.2 Objective of the Research Work	70
6.3 Organization of Part 2 of the Thesis	71
Chapter 7	72
7 Literature Review	72
7.1 Precious Metals and Recovery of Precious Metals	72
7.1.1 Precious Metals	72
7.1.2 Recovery of Precious Metals	73
7.2 Gold Bioadsorption and Bioadsorbents of Gold	75
7.2.1 Gold Bioadsorption	75
7.2.2 Bioadsorbents of Gold	77
7.2.2.1 Algae	77
7.2.2.2 Fungi	78
7.2.2.3 Yeasts	78
7.2.2.4 Plant Biomass	79
7.3 Cellulose Based Bioadsorbents like Paper and Cloth	81
7.3.1 Paper	81
7.3.2 Cloth	82
Chapter 8	83

8 Materials and Methods	83
8.1 Materials	83
8.2 Preparation of Adsorption Gel from Cloth and Paper	83
8.3 Measurement and Analysis	84
8.4 Batch Adsorption Test	85
8.5 Kinetic Studies	86
8.6 Isotherm and Kinetic Models	87
8.7 XRD Analysis	88
8.8 FT-IR Analysis	88
8.9 Scanning Electron Microscope (SEM) Analysis	89
Chapter 9	90
9 Results and Discussion	90
9.1 Influence of pH for the Metal Adsorption	90
9.2 Effect of pH on Metal Adsorption	91
9.3 Effect of Solid/Liquid Ratio on Metal Adsorption	93
9.4 Adsorption Isotherms	95
9.5 Kinetic Studies	104
9.6 Effect of Increasing Solid/Liquid Ratio to Increase the Reaction Time	106
9.7 Proposed Mechanism of Metal Adsorption	109
9.8 XRD Analysis Result	110
9.9 FT-IR Analysis Result	112
9.10 SEM Analysis Result	114

9.11 Research Findings	122
Chapter 10	124
10 Conclusion and Recommendation	124
10.1 Conclusion	124
10.2 Proposals for the Future Work	125
REFERENCES	126
APPENDIXES	140

LIST OF TABLES

Table 2.1 : Orange peel composition (Percent on dry basis).	18
Table 4.1: Amount of adsorption ($q/\text{mol kg}^{-1}$) and percentage of adsorption (R) of different metal ions in different water sample by Ca^{2+} form SOJR.	40
Table 4.2: Pseudo-first-order, pseudo-second-order, Langmuir, Freundlich model parameters for metal bioadsorption equilibrium on Ca^{2+} form SOJR.	46
Table 7.1: Recovery methods of gold.	73
Table 7.2: Recovery method of other precious metals.	74
Table 7.3: Bioadsorbents of gold.	77
Table 7.4: Bioadsorption of gold using different adsorbents.	79
Table 7.5: The natural composition of native wood and the pulps.	81
Table 9.1: Thermodynamic parameters for the adsorption of Au(III) on cloth adsorbent gel.	101
Table 9.2: Thermodynamic parameters for the adsorption of Au (III) on paper adsorbent gel.	102
Table A1: ICP results on water samples of different metal concentrations	141
Table A2: ICP results on water samples of different solid liquid ratio	144
Table A3: ICP results on water samples of different pH	145
Table A4: ICP results on water samples at different time	146
Table B1: ICP results on samples of different HCL concentrations	148
Table B2: ICP results on water samples of different pH	153

Table B3: ICP results on water samples of different time	156
Table B4: ICP results on samples of different solid/liquid ratio	158
Table B5: ICP results on samples of different time at different solid/liquid ratio	160

LIST OF FIGURES

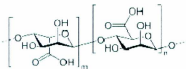
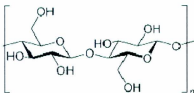
Figure 2.1: Process block diagram of metal extraction.	9
Figure 2.2: Roman Portal with acid mine drainage – Spain.	10
Figure 2.3: Saponification of orange juice residue.	19
Figure 2.4: Bruker TENSOR 27 infrared spectrometer.	22
Figure 2.5: Rigaku Ultima IV X-ray diffractometer.	24
Figure 2.6: Schematic diagram of XRD theory.	25
Figure 2.7: FEI Quanta 400 environmental SEM.	26
Figure 3.1: Synthetic route of SOJR.	31
Figure 4.1: Removal of metal ions from aqueous solution on the Ca^{2+} -form SOJR as a function of initial concentration.	40
Figure 4.2(a): Removal of lead(Pb) ions from aqueous solution on the Ca^{2+} -form SOJR as a function of solid/liquid ratio.	41
Figure 4.2(b): Removal of copper(Cu) ions from aqueous solution on the Ca^{2+} -form SOJR as a function of solid/liquid ratio.	42
Figure 4.2(c): Removal of zinc(Zn) ions from aqueous solution on the Ca^{2+} -form SOJR as a function of solid/liquid ratio.	43
Figure 4.3: Removal of metal ions from aqueous solution on the Ca^{2+} -form SOJR as a function of equilibrium pH.	44
Figure 4.4 : Adsorption isotherms of some metal ions at pH 3.5.	47
Figure 4.5: (a) Adsorption isotherms at different pH, and (b) corresponding Langmuir	

Plots for Cu(II).	48
Figure 4.6: (a) Adsorption isotherms at different pH, and (b) corresponding Langmuir	
Plots for Zn(II).	49
Figure 4.7: (a) Adsorption isotherms at different pH, and (b) corresponding Langmuir	
Plots for Pb(II).	50
Figure 4.8: Adsorption kinetics for different acid mine sample of different AMD sample.	51
Figure 4.9: Adsorption mechanism of metal cations on pectin.	52
Figure 4.10: XRD pattern of a SOJR containing Pb.	53
Figure 4.11: FT-IR Analysis of the SOJR.	55
Figure 4.12: FT-IR Spectrum of SOJR after metal adsorption.	56
Figure 4.13: SEM photograph of SOJR.	57
Figure 4.14: SEM photograph of SOJR after metal adsorption.	58
Figure 4.15 : X-ray analysis of Ca^{2+} -form SOJR by SEM.	59
Figure 4.16: X-ray analysis of Ca^{2+} -form SOJR with metals by SEM.	60
Figure 7.1: Chemical structure of cotton.	82
Figure 8.1: Synthetic route of cross-linked adsorption gel.	84
Figure 9.1: Adsorption of metals ions on (a) cloth juice, (b) paper juice as a function of hydrochloric acid concentration.	91
Figure 9.2: Adsorption of metal ions on (a) cloth juice, (b) paper juice as a function of pH.	92
Figure 9.3: Removal of metal ions from aqueous solution on the a) cloth juice, b) paper gel as a function of solid/liquid ratio.	94
Figure 9.4: Adsorption rate of Au(III) by the adsorption gel at different temperatures	96

Figure 9.5: Adsorption rate of Au (III) by the adsorption juice at different temperatures. Pseudo-first order plot.	97
Figure 9.6: Adsorption rate of Au (III) by the adsorption juice at different temperatures. Arrhenius plot.	98
Figure 9.7: Adsorption isotherms at different temperature (a) Langmuir plots (b) Van's Hoff plot for cloth gel.	99
Figure 9.8: Adsorption isotherms at different temperature (a) Langmuir plots and (b) Van's Hoff plot for paper gel.	100
Figure 9.9: Adsorption isotherms of Au(III) onto cotton gel at different temperatures. (a) For cloth and b) for paper.	103
Figure 9.10: Adsorption kinetics of different metal a) on cloth gel and (b) on paper gel.	105
Figure 9.11: Adsorption kinetics at different sample of different solid liquid ratio.(a) on cloth gel and (b) on paper gel.	106
Figure 9.12: Adsorption isothems at different samples of higher solid liquid ratio.(a) on cloth gel and (b) on paper gel.	107
Figure 9.13 : Adsorption mechanism of Au(III) ions on cellulose based gel.	109
Figure 9.14: XRD pattern of a cloth adsorbent gel containing Au(III).	110
Figure 9.15: XRD pattern of a paper adsorbent gel containing Au(III).	111
Figure 9.16: FT-IR Spectrum of cloth adsorbent gel before and after gold adsorption.	112
Figure 9.17: FT-IR Spectrum of paper adsorbent gel before and after gold adsorption.	113
Figure 9.18: SEM photograph of cloth adsorbent gel before gold adsorption.	114
Figure 9.19: SEM photograph of cloth adsorbent gel after gold adsorption. Mag: 4000X.	115
Figure 9.20: SEM photograph of cloth adsorbent gel after gold adsorption.	

Mag:10000X.	116
Figure 9.21: EDX analysis of cloth adsorbent gel with gold by SEM.	117
Figure 9.22: SEM photograph of paper adsorbent gel before gold adsorption.	118
Figure 9.23: SEM photograph of paper adsorbent gel after gold adsorption.Mag:1100X.	119
Figure 9.24: SEM photograph of paper adsorbent gel after gold adsorption. Mag:10000X.	120
Figure 9.25: EDX analysis of paper adsorbent gel with gold by SEM.	121

LIST OF ABBREVIATIONS

Ag	Silver
AGU	Anhydroglucose unit
Alginic acid	
AMD	Acid Mine Drainage
Au	Gold
BSE	Back-scattered electrons
C	Celsius
Ca	Calcium
CBO	Cross Beam Optics
CCDs	Charge coupled devices
C-CART	Centre of Chemical analysis, Research and Training
Cd	Cadmium
Cellulose	
cm	Centimeter
Co	Cobalt
Cu	Copper

DP	degree of polymerisation
EPA	Environmental Protection Agency
EDX	Energy dispersive x-ray
FEG	Field emission guns
h	Hour
ICP-AES	Inductively coupled plasma atomic emission spectroscopy
ICP-OES	Inductively coupled plasma optical emission spectrometry
ISO	International organisation of standardization
Kg	Kilogram
L	Litre
M	Molar
MAF-IIC	Micro Analysis Facility-INCO Innovation Centre
mg	Milligram
mL	Millilitre
mM	Milimolar
µm	Micrometer
Ni	Nickel
Pb	Lead
Pd	Palladium
Pectic acid	α-D-Polygalacturonic acid, $(C_6H_{10}O_6)_n$
pH	-log[H]
ppm	Parts per million

Pt	Platinum
rpm	Revolutions per minute
SEM	Scanning electron microscope
S/L	Solid-liquid
SOJR	Saponified Orange Juice Residue
TERRA	The Earth Resources Research and Analysis
UV-Vis	Ultraviolet-visible
USEPA	United States Environmental Protection Agency
XRD	X-ray diffraction
Zn	Zinc

LIST OF SYMBOLS

Symbol	Description	Unit
θ	Angle	degree
λ	Wavelength	harz
d	Diameter	centimeter
q	Amount of adsorption	molar/kilogram
C_0	Initial Concentration	Molar
C_e	Equilibrium Concentration	molar
W	Weight	Kilogram
V	Volume	Cubic centimeter
R	Rate of adsorption	
q_e	Equilibrium metal adsorption	molar/kilogram
$q_{m\max}$	Maximum metal adsorption	molar/kilogram
b	Langmuir constant	
K^f, n	Freundlich constants	
t	Time	Minute
K_1	adsorption rate constant of the pseudo-first-order equation	l/minute
K_2	adsorption rate constant of the pseudo-second-order equation	l/minute
R^2	Correlation coefficient of the pseudo-second-order equation	

LIST OF APPENDICES

Appendix A	Experimental Result for Removals of Heavy Metals from Acid Mine Drainage (AMD) using Bioadsorbent from Orange Waste	140
Appendix B	Experimental Results for Recovery of Gold from Synthetic Solution using Cellulose base Bioadsorbents from Paper and Cloth	146

PART 1

Removals of Heavy Metals from Acid Mine Drainage (AMD) using
Bioadsorbent from Orange Waste

CHAPTER 1

1 Introduction

1.1 Background

Acid mine drainage (AMD) refers to the outflow of acidic water from metal mines or coal mines. AMD is a strongly acidic solution containing high amounts of heavy metals and sulphate and consequently threatens groundwater quality. It is generated by the chemical and biological oxidation of pyrite, pyrrhotite and other metal sulphides in mine waste heaps or in tailings from sulfidic ore processing.

Waters draining from active and, in particular, abandoned mines and mine wastes are often net acidic. Such waters typically pose an additional risk to the environment because they often contain elevated concentrations of metals such as iron, aluminum and manganese, and possibly other heavy metals and metalloids. In 1989, it was estimated that 19,300 km of streams and rivers, and 72,000 hectare of lakes and reservoirs worldwide had been seriously damaged by mine effluents, although the true scale of the environmental pollution caused by mine water discharges is difficult to assess accurately. AMD may form in the underground workings of deep mines, although this is generally of minor importance when a mine is in active production and water tables are kept artificially low by pumping. However, when mines are closed and abandoned, and the pumps turned off, the rebound of the water table can lead to contaminated groundwater being discharged. The results can be catastrophic such as the events at the Wheal Jane mine in 1992 when a range of contaminants entered the environment (Younger et al., 2004; Neal et al., 2004). Since the water that refills the mine dissolves any acidic salts that have built

up on the pore spaces of the exposed walls and ceilings of the underground chambers, this initial drainage water tends to be more potentially polluting in terms of acidity and metal content than AMD that is discharged subsequently (Clarke, 1995).

Acidic metal-rich waters may also form in spoil headstand mineral tailings, essentially by the same biologically driven reactions as in mine shafts. Due to the more disaggregated nature of the acid-generating minerals in these waste materials, AMD that flows from them may be more aggressive than that which discharges from the mine itself. Another important consideration here is the potential long-term pollution problem, as production of AMD may continue for many years after mines are closed and tailing dams are decommissioned. Although the generic term acid mine drainage is used frequently to describe mine water discharges, the pH of these waters may be above 6, particularly at the point of discharge where dissolved oxygen concentrations are frequently very low. Some AMD streams remain neutral-to-alkaline, while others show a marked decline in pH as they oxygenate.

Known as Lucky Strike, the mine in Buchans, Newfoundland was a prime source of lead, zinc, copper, silver and gold for Newfoundland. Over 16 tons of high-grade ore was produced while it was in operation. The mine was established in 1905 and became fully functional in the 1920s. The mine hasn't been operational since 1984. Soil tests from around that mine found dangerously high levels of lead, along with nine other toxic substances. Lead is a metallic pollutant that is toxic to numerous bodily organs and tissues, including the heart, bones, intestines, kidneys, reproductive system and nervous system. It is especially toxic to children and may cause permanent learning and behavioral disorders. Symptoms include abdominal pain, headaches, anemia and irritability. Extreme or prolonged exposure could cause seizures, coma or death (Dearing, 2009).

The conventional technologies for the removal of toxic metals from the wastewater include ion exchange, chemical reduction, chemical precipitation, electrochemical treatment, membrane separation etc. In general, most are expensive and are ineffective when heavy metals are present in the wastewater at low concentrations. Therefore an efficient and cost-effective treatment method is required to treat large volumes of industrial heavy metal-bearing wastewaters (Leusch and Volesky 1995; Volesky 2001).

Biosorption removes metal ions by biological materials and biomaterials and have been considered as potentially important sorbents for heavy metal removal. In the past decades, biosorption, bioprecipitation, and uptake by biopolymers derived from agricultural wastes or microbes have emerged as techniques to provide alternative and/or additive processes for conventional physical and chemical methods for removing toxic ions from wastewater (Jamode et al., 2003; Hussein et al., 2005). Hence, a lot of effort has been made on screening of efficient biomass types, their preparation and biosorption mechanism. The uptake of heavy metals by biomass can in some cases reach up to 50% of the biomass dry weight. New biosorbents can be manipulated for better efficiency and multiple re-use to increase their economic attractiveness (Regine and Boya, 2000). Of particular interest are the abundant biomass generated as a waste by-product of large-scale industrial processes and vegetable biomass, such as marine algae (Luo et al., 2006), rice husk (Chockalingamand Subramanian 2006), sawdust (Larous et al., 2005), crop milling waste (Saeed et al., 2005), corncob (Leyva-Ramos et al., 2005), cellulose/chitin beads (Zhou et al., 2005), etc.

In previous, researchers have reported the adsorptive removal of heavy metals using gels of alginic acid and pectic acid, which show remarkable separation features for heavy metal ions (Yano and Inoue, 1997; Dhakal et al., 2005). The selectivity of these gels for some specific metal

ions is much superior to commercially available chelating resins and adsorption capacities are competitive. Although the physical or mechanical strength of these gels may be much weaker than the synthetic resins, they are environmental benign, biodegradable and free from post-treatment problems. Pectic acid and alginic acid gels exhibit excellent adsorption behavior for heavy metals; however, the cost of extracting these polysaccharides from their corresponding feed materials to produce the adsorption gels is high.

Large quantities of various biomass wastes are being generated in agriculture, forestry and fisheries. Some of these biomass wastes contain various natural materials with interesting functions such as pectic acid and alginic acid. If these biomass wastes exhibit the adsorption behaviors for metal ions similar to the pectic acid and alginic acid gels, it would be possible to use them successfully at very low price, as there is no need to extract the pectic acid or alginic acid. Several researchers (Yano et al., 2001; Dhakal et al., 2005) attempted to prepare another type of adsorption gel from orange juice residue, by a much cheaper and simpler method without using any organic cross linking reagents so as to avoid the problems of waste treatment after cross linking based on the presumption that the adsorption gel is not reused after adsorption, that is, from economical point of view it is used only once for adsorption. In those work, researchers have investigated in detail the removal of Lead (Pb(II)), Cadmium (Cd(II)), Zinc (Zn(II)), Nickel (Ni(II)) and Cobalt (Co(II)) in hydrochloric systems by orange waste. Orange waste cellulose was chosen as bioadsorbent due to its special structure, insolubility in water, chemical stability and local availability.

1.2 Objective of the Research Work

The main objective of this work is to find a sustainable process to remove heavy metals from acid mine drainage using local biomass like Saponified Orange Juice Residue (SOJR).

In this work, I tried to investigate the effect of orange waste to uptake the heavy metal like Pb(II), Cu(II) and Zn(II) from the acid mine drainage water. I made some synthetic solution keeping same concentration of heavy metal like AMD sample water taken from Buchans and reacted with SOJR and measured the amount of metal uptake by the orange waste. I used solutions of different concentration and different pH level to measure the effect of these conditions on uptake. Along with that I measured the effect of solid liquid ratio, temperature and time on this reaction.

I also investigated the kinetic studies and isotherm properties of this extraction process and developed a model for this. The micro level investigation like X-ray diffraction (XRD) and Fourier Transform Infra red (FT-IR) analysis were done to prove the effect of the bioadsorbent on metals. I also tried to see the micro image of bonding sites of the adsorbents by Scanning Electron microscopy analysis.

1.3 Organization of the part of thesis

This part of thesis has been organized as follows

Chapter 1 provides the key research introduction and objectives followed by the organization of this part of the thesis.

Chapter 2 provides a details literature review. The literature review starts with a general discussion of mining and AMD and has been narrowed down to adsorption and with elaborate description of bioadsorbents like SOJR.

Chapter 3 describes the detailed experimental steps performed in this research part with a brief description of the adsorbents.

Chapter 4 is the most important part of this part of the thesis, which describes the research findings and presents elaborate discussion with different parts of the results of this study.

Chapter 5 describes the research conclusion along with the recommendations for future this research.

CHAPTER 2

2 Literature Review

2.1 Mining and Acid Mine Drainage

2.1.1 Mining

Mining refers to the processes, occupations, industries related to the extraction of valuable minerals or other geological materials from the earth, from an ore body, vein or coal seam. Materials recovered by mining include base metals, precious metals, iron, uranium, coal, diamonds, limestone, oil shale, rock salt and potash. Any material that cannot be grown through agricultural processes, or created artificially in a laboratory or factory, are found by mining. Mining in a wider sense comprises the extraction of any non-renewable resource such as petroleum, natural gas, or even water (Mining, 2012).

Extractive metallurgy is the practice of extracting metal from ore, purifying it, and recycling it. Most metals found in the Earth's crust exist as oxide and sulfide minerals. These compounds must be reduced to liberate the desired metal. There are two methods of reduction: electrolytic and chemical. Mineral processing involves manipulating the particle size of solid raw materials and separating valuable materials from materials of no value. The schematic metallurgical process is given in Figure 2.1.

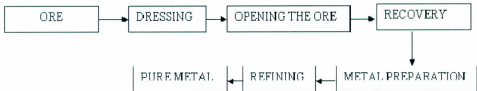


Figure 2.1: Process block diagram of metal extraction.

Extractive metallurgy can be divided into two parts, pyrometallurgy and hydrometallurgy. Pyrometallurgy, or the dry process, involves the thermal treatment of minerals and metallurgical ores and concentrates to bring about physical and chemical transformations in the materials to enable the recovery of valuable metals. Pyrometallurgical treatment may produce saleable products such as pure metals, or intermediate compounds or alloys, suitable as feed for further processing. By contrast, hydrometallurgy involves the use of aqueous chemistry for the recovery of metals from ores, concentrates, and recycled or residual materials. Sometimes metal are extracted by a combination of the two methods depending on the chemical nature of the metal. But in both cases 100 % metal cannot be extracted.

2.1.2 Acid Mine Drainage

Acid mine drainage (AMD) is formed by the natural oxidation of sulphide minerals when exposed to air and water. Activities that involve the excavation of rock with sulphide minerals, such as metal and coal mining, accelerate the process. The drainage produced from the oxidation process may be neutral to acidic, with or without dissolved heavy metals, but always contains sulphate. AMD results from a series of reactions and stages that typically proceed from near neutral to more acidic pH conditions. The AMD formation process can continue to produce

impacted drainage for decades or centuries after mining has ceased, as illustrated by a portal dating from the Roman era in Spain (Figure 2.2).



Figure 2.2: Roman Portal with Acid mine drainage – Spain.(Acid mine drainage,2012)

Although pyrite is by far the dominant sulphide responsible for the generation of acidity, different ore deposits contain different types of sulphide minerals. Not all of these sulphide minerals when being oxidized generate acidity. As a general rule, iron sulphides (pyrite, marcasite, pyrrhotite), sulphides with molar metal/sulphur ratios < 1, and sulfosalts (e.g., enargite) generate acid when they react with oxygen and water. Sulphides with metal/sulphur ratios = 1 (e.g., sphalerite, galena, chalcopyrite) tend not to produce acidity when oxygen is the oxidant. However, when aqueous ferric iron is the oxidant, all sulphides are capable of generating acidity. Therefore, the acid generation potential of an ore deposit or mine waste generally depends on the amount of iron sulphide present (Acid mine drainage, 2012).

2.1.2.1 Heavy Metal in Acid Mine Drainage

Acid waters dissolve many of the minerals present in ore causing iron and potentially toxic elements, such as copper, cadmium, lead and zinc, to be solubilised. The waters are then discharged into a stream and into the sea. The acidity can be neutralised slowly by the stream or more rapidly by the ocean, but not before some adverse effects may have occurred.

While copper and zinc are essential trace elements for plant and animal life including humans, they are toxic at high doses. There are no known beneficial properties of cadmium. It is highly toxic to plants, animals and humans and many aquatic species are very sensitive to cadmium. When these minerals present in bioavailable forms, bioaccumulation has been observed in both aquatic and terrestrial organisms (Savinov, 2003).

Heavy metal pollution is caused when such metals such as arsenic, cobalt, copper, cadmium, lead, silver and zinc contained in excavated rock or exposed in an underground mine come in contact with water. Metals are leached out and carried downstream as water washes over the rock surface. Although metals can become mobile in neutral pH conditions, leaching is particularly accelerated in low pH conditions such as those created by Acid Mine Drainage.

2.1.2.2 Pollution by Lead

Lead and lead compounds are generally toxic pollutants. Lead(II) salts and organic lead compounds are most harmful ecotoxicologically. Lead salts are attributed to water hazard class 2, and are consequently harmful. The same applies to lead compounds such as lead acetate, lead oxide, lead nitrate, and lead carbonate. Lead limits plant chlorophyll synthesis. Nevertheless, plants can sustain high levels of lead (up to 500 ppm) from soils. Concentrations higher than 500

ppm negatively influence plant growth. Through plant uptake, lead enters food chains. Consequently, lead pesticide application is prohibited in most countries. Lead accumulates in organisms, sediments and sludge.

The human body contains approximately 120 mg of lead. About 10-20% of this lead is absorbed by the intestines. Symptoms of overexposure to lead include colics, skin pigmentation and paralysis. Generally, effects of lead poisoning are neurological or teratogenic. Organic lead causes necrosis of neurons. Inorganic lead causes axonal degeneration and demyelination. Both species of lead may cause cerebral oedema and congestion. Symptoms of lead poisoning include lower IQs, behavioral changes and concentration disorder. Lead accumulates in leg tissue. The most severe type of lead poisoning causes encephalopathy. Lead toxicity is induced by lead ions reacting with free sulphydryl groups of proteins, such as enzymes. These are deactivated. Furthermore, lead may interact with other metal ions. Organic lead compounds are absorbed quicker, and therefore pose a greater risk. Organic lead derivates may be carcinogenic. Women are generally more susceptible to lead poisoning than men. Lead causes menstrual disorder, infertility and spontaneous abortion, and it increases the risk of stillbirths. Foetuses are more susceptible to lead poisoning than mothers, and generally foetuses protect mothers from lead poisoning by adsorbing the excess lead in the mother's body. In the past, lead was applied as a measure of birth control, for example as a spermicidal, and to induce abortion. Children may absorb a larger amount of lead per unit body weight than adults (up to 40%) and are consequently more susceptible to lead poisoning (Lead Poisoning, 2012).

2.1.2.3 Pollution by Copper

Copper in water exists as a divalent ion, Cu²⁺. Levels over 0.05 mg/L are not naturally encountered in groundwater. Copper is a metallic element that is essential to human health. Too little is unhealthy and too much can lead to copper poisoning. The body cannot synthesize copper so the human diet must supply regular amounts for absorption. The daily requirement is about 2 milligrams of copper intake per day to maintain a balance of 75-100 mg in the adult body.

The United States Environmental Protection Agency (USEPA) has found that copper potentially causes the following health effects when people are exposed to it at high levels. Short periods of exposure can cause gastrointestinal disturbance, including nausea and vomiting. According to the EPA, use of copper drinking water that contains over 1.3 mg of copper per liter of water (mg/L) over a long period of time, could cause liver or kidney damage. People with Wilson's disease, a hereditary disorder that permits increased intestinal absorption of copper and accumulation of copper in various organs such as the brain, liver, kidney, and cornea may be more sensitive than others to the effects of copper contamination. There is inadequate evidence to state whether or not copper has the potential to cause cancer from a lifetime exposure in drinking water (Copper Toxicity, 2012).

2.2 Removal of Heavy Metal from Acid Mine Drainage

AMD can be neutralized using chemicals like lime, calcium carbonate, hydrated lime, caustic soda and soda ash. The neutralization process results in the production of voluminous sludge and this sludge disposal poses a further environmental problems additional costs (Fiset et al., 2003). The high cost of conventional clean up technologies has produced economic pressure on the society and has caused engineers to search for creative, cost effective and environmentally sound ways to treat AMD. In the past few decades, therefore, research efforts have been directed towards wetlands as an alternative low cost means of removing heavy metals from AMD as well as domestic, commercial and industrial waste water (Matagi et al., 1998 ; Fyson et al., 1994). Both natural and artificially constructed wetlands offer an efficient treatment technology with minimum input, low investment costs, low operating costs and no external energy input (Dunbabin and Bowmer, 1992; Kleinmann and Hedin, 1993; Tam and Wong, 1994; Matagi et al., 1998; Kalin, 2004; Woulds and Ngwenya, 2004).

2.2.1 Adsorption

In sediments heavy metals are adsorbed to the soil particles by either cation exchange or chemisorption. Patrick and Verloo (1998) reported that heavy metals are adsorbed to the clay and organic matter by electrostatic attraction. Cation exchange involves the physical attachment of cations to the surfaces of clay and organic matter by electrostatic attraction. Once the heavy metals are adsorbed on to humic or clay colloids, heavy metals will remain as metal atoms, unlike organic pollutants, which will ultimately decompose. Their speciation may change with time as the sediment conditions change (Berner, 1980; Kadlec and Keoleian, 1986; Drever, 1988; Groudev et al., 1999; Batty et al., 2002; Wiebner et al., 2005).

Many constituents of wastewater and run off exist as cations, including most of the trace metals such as Cu, Zn, Pb, Ni and Cd. The capacity of soils for retention of cations, expressed as cation exchange capacity generally increases with certain substrates with increasing clay and organic matter content. Chemisorption represents a stronger and more permanent form of bonding than cation exchange. The adsorption capacity by cation exchange or non-specific adsorption depends upon the physico-chemical environment of the medium, the properties of the metals concerned and the concentration and properties of other metals and soluble ligands present (Alloway 1992; Alloway and Ayre, 1993; Thomas et al., 1996; Matagi et al., 1998).

More than 50% of heavy metals can be easily adsorbed onto particulate matter and thus be removed from the water component by sedimentation (Muller, 1988). Lead and copper generally tend to be adsorbed most strongly and zinc, nickel and cadmium are usually held weakly which implies that these metals are likely to be more liable and bio available (Alloway, 1990). The adsorption of metals varies with the fluctuation of pH in the outflow water (Machemer and

Wildeman, 1992). According to Wood (2004) the precipitated hydroxides also act as adsorption sites for phytotoxic metals present in the water.

2.2.2 Adsorbents

Adsorbents are usually used in the form of spherical pellets, rods, moldings, or monoliths with hydrodynamic diameters between 0.5 and 10 mm. They must have high abrasion resistance, high thermal stability and small pore diameters, which results in higher exposed surface area and hence high surface capacity for adsorption. The adsorbents must also have a distinct pore structure which enables fast transport of the gaseous vapors.

2.3 Bioadsorption and Bioadsorbents

Bioadsorption is a physiochemical process that occurs naturally in certain biomass allowing it to passively concentrate and bind contaminants onto its cellular structure. Though using biomass in environmental cleanup has been in practice for a while, scientists and engineers are hoping this phenomenon will provide an economical alternative for removing toxic heavy metals from industrial wastewater and aid in environmental remediation.

Pollution interacts naturally with biological systems. It is currently uncontrolled, seeping into any biological entity within the range of exposure. The most problematic contaminants include heavy metals, pesticides and other organic compounds, which can be toxic to wildlife and humans in small concentration. There are existing methods for remediation, but they are either expensive or ineffective. However, an extensive body of research has found that a wide variety of commonly discarded waste, including eggshells, bones, peat, fungi, seaweed, yeast and carrot

peels can efficiently remove toxic heavy metal ions from contaminated water. Ions from metals like mercury can react in the environment to form harmful compounds like methyl mercury, which is known to be toxic in humans. In addition, adsorbing biomass, or bioadsorbents, can also remove other harmful metals such as: arsenic, lead, cadmium, cobalt, chromium and uranium. Bioadsorption may be used as an environmentally friendly filtering technique. There is no doubt that the world could benefit from more rigorous filtering of harmful pollutants created by industrial processes and all-around human activity.

The idea of using biomass as a tool in environmental cleanup has been around since the early 1900's when Arden and Lockett (Aden and Lockett, 1914) discovered that certain types of living bacteria cultures were capable of recovering nitrogen and phosphorus from raw sewage when it was mixed in an aeration tank. This discovery became known as the activated sludge process which is based on the concept of bioaccumulation and is still widely used in wastewater treatment plants today. It was not until the late 1970s, however when scientists noticed the sequestering characteristic in dead biomass, which resulted in a shift in research from bioaccumulation to bioadsorption.

2.4 Orange Peel

The characterization of the orange peel started with the determination of its elemental composition, which resulted to be the following (wt %): C, 45.1; N, 1.04; H, 5.95; S, 0.00; and O, 44.4. Meanwhile, the determination of metals showed the highest contents (mg/kg) for K (8,297), Ca (5,457), Mg (827), and Na (506). All of these metals are usually part of the culture media recommended for the cultivation of several microorganisms. Besides, other fundamental

metals were shown to be present in smaller amounts (mg/kg): Zn, 4.95; Mn, 4.60; Fe, 15.1; Al < 105; Ni < 20; Cu, 6.00; Cr < 10.

Table 2.1: Orange peel composition (Percent on dry basis) (Rivas et al., 2008)

Compound	%
soluble sugars	16.9
Starch	3.75
Fiber	
Cellulose	9.21
hemicelluloses	10.5
Lignin	0.84
Pectins	42.5
Ashes	3.50
Fats	1.95
Protein	6.50
other compounds	4.35

Table 2.1 shows the overall orange peel composition: soluble sugars, 16.9 wt %; starch, 3.75 wt %; fiber (cellulose 9.21 wt %; hemicelluloses, 10.5 wt %; lignin 0.84 wt %; and pectins, 42.5 wt %), ashes, 3.50 wt %; fats, 1.95 wt %; and proteins, 6.50 wt %.

Orange waste consists of cellulose, hemicellulose, pectin, limonene and many other low molecular weight compounds. In addition to free carboxyl groups, pectin also possesses methyl ester groups in its polymeric chain. Such methyl ester groups are saponified with calcium hydroxide under highly alkaline conditions to convert them into carboxyl groups according to the following reaction:

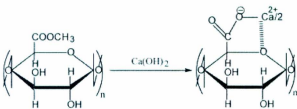


Figure 2.3: Saponification of orange juice residue

2.5 Chemical Analysis Device

2.5.1 Chemical Analysis by ICP-OES

Inductively coupled plasma atomic emission spectroscopy (ICP-AES), also referred to as inductively coupled plasma optical emission spectrometry (ICP-OES), is an analytical technique used for the detection of trace metals. It is a type of emission spectroscopy that uses the inductively coupled plasma to produce excited atoms and ions that emit electromagnetic radiation at wavelengths characteristic of a particular element. The intensity of this emission is indicative of the concentration of the element within the sample.

2.5.1.1 Mechanism

The ICP-AES is composed of two parts: the ICP and the optical spectrometer. The ICP torch consists of 3 concentric quartz glass tubes. The output or "work" coil of the radio frequency (RF) generator surrounds part of this quartz torch. Argon gas is typically used to create the plasma.

When the torch is turned on, an intense electromagnetic field is created within the coil by the high power radio frequency signal flowing in the coil. This RF signal is created by the RF generator which is, effectively, a high power radio transmitter driving the "work coil" the same way a typical radio transmitter drives a transmitting antenna. The argon gas flowing through the torch is ignited with a Tesla unit that creates a brief discharge arc through the argon flow to initiate the ionization process. Once the plasma is "ignited", the Tesla unit is turned off.

The argon gas is ionized in the intense electromagnetic field and flows in a particular rotationally symmetrical pattern towards the magnetic field of the RF coil. Stable, high temperature plasma of about 7000 K is then generated as the result of the inelastic collisions created between the neutral argon atoms and the charged particles.

A peristaltic pump delivers an aqueous or organic sample into a nebulizer where it is changed into mist and introduced directly inside the plasma flame. The sample immediately collides with the electrons and charged ions in the plasma and is itself broken down into charged ions. The various molecules break up into their respective atoms which then lose electrons and recombine repeatedly in the plasma, giving off radiation at the characteristic wavelengths of the elements involved.

In some designs, a shear gas, typically nitrogen or dry compressed air is used to 'cut' the plasma at a specific spot. One or two transfer lenses are then used to focus the emitted light on a diffraction grating where it is separated into its component wavelengths in the optical spectrometer. In other designs, the plasma impinges directly upon an optical interface which consists of an orifice from which a constant flow of argon emerges, deflecting the plasma and providing cooling while allowing the emitted light from the plasma to enter the optical chamber. Still other designs use optical fibers to convey some of the light to separate optical chambers.

Within the optical chamber(s), after the light is separated into its different wavelengths (colors), the light intensity is measured with a photomultiplier tube or tubes physically positioned to "view" the specific wavelength(s) for each element line involved, or, in more modern units, the separated colors fall upon an array of semiconductor photodetectors such as charge coupled devices (CCDs). In units using these detector arrays, the intensities of all wavelengths (within the system's range) can be measured simultaneously, allowing the instrument to analyze for every element to which the unit is sensitive all at once. Thus, samples can be analyzed very quickly.

The intensity of each line is then compared to previously measured intensities of known concentrations of the elements, and their concentrations are then computed by interpolation along the calibration lines.

In addition, special software generally corrects for interferences caused by the presence of different elements within a given sample matrix.

2.5.2 Chemical Analysis by FT-IR

Fourier transform infrared spectroscopy (FTIR) is a technique which is used to obtain an infrared spectrum of absorption, emission, photoconductivity or Raman scattering of a solid, liquid or gas. An FTIR spectrometer simultaneously collects spectral data in a wide spectral range. This confers a significant advantage over a dispersive spectrometer which measures intensity over a narrow range of wavelengths at a time. FTIR has made dispersive infrared spectrometers all but obsolete, opening up new applications of infrared spectroscopy.



Figure 2.4: Bruker TENSOR 27 infrared spectrometer.

The goal of any absorption spectroscopy is to measure how well a sample absorbs light at each wavelength. The most straightforward way to do this, the "dispersive spectroscopy" technique, is to shine a monochromatic light beam at a sample, measure how much of the light is absorbed, and repeat for each different wavelength.

Fourier transform spectroscopy is a less intuitive way to obtain the same information. Rather than shining a monochromatic beam of light at the sample, this technique shines a beam containing many different frequencies of light at once, and measures how much of that beam is absorbed by the sample. Next, the beam is modified to contain a different combination of

frequencies, giving a second data point. This process is repeated many times. Afterwards, a computer takes all these data and works backwards to infer what the absorption is at each wavelength.

The beam described above is generated by starting with a broadband light source—one containing the full spectrum of wavelengths to be measured. The light shines into a certain configuration of mirrors, called a Michelson interferometer, which allows some wavelengths to pass through but blocks other. The beam is modified for each new data point by moving one of the mirrors; this changes the set of wavelengths that pass through.

As mentioned, computer processing is required to turn the raw data (light absorption for each mirror position) into the desired result (light absorption for each wavelength). The processing required turns out to be a common algorithm called the Fourier transform.

2.5.3 Chemical Analysis by XRD

About 95% of all solid materials can be described as crystalline. When X-rays interact with a crystalline substance, one gets a diffraction pattern. In 1919 A.W.Hull gave a paper titled, “A New Method of Chemical Analysis”. Here he pointed out that “....every crystalline substance gives a pattern; the same substance always gives the same pattern; and in a mixture of substances each produces its pattern independently of the others.”. The X-ray diffraction pattern of a pure substance is, therefore, like a fingerprint of the substance. The powder diffraction method is thus ideally suited for characterization and identification of polycrystalline phases. Today about 50,000 inorganic and 25,000 organic single components, crystalline phases, and diffraction patterns have been collected and stored on magnetic or optical media as standards. The main use of powder diffraction is to identify components in a sample by a search/match procedure.

Furthermore, the areas under the peak are related to the amount of each phase present in the sample.

2.5.3.1 Theoretical Considerations

If we use the three dimensional diffraction grating as a mathematical model, the three indices h , k , l become the order of diffraction along the unit cell axes a , b and c respectively.

It should now be clear that, depending on what mathematical model we have in mind, we use the terms X-ray reflection and X-ray diffraction as synonyms.

Let us consider an X-ray beam incident on a pair of parallel planes $P1$ and $P2$, separated by an interlinear spacing d .



Figure 2.5: Rigaku Ultima IV X-ray diffractometer.(XRD 2012)

The two parallel incident rays 1 and 2 make an angle (θ) with these planes. A reflected beam of maximum intensity will result if the waves represented by $1'$ and $2'$ are in phase. The difference in path length between 1 to $1'$ and 2 to $2'$ must then be an integral number of wavelengths, (λ). We can express this relationship mathematically in Bragg's law.

$$2d \cdot \sin T = n \cdot A$$

The process of reflection is described here in terms of incident and reflected (or diffracted) rays, each making an angle Θ with a fixed crystal plane. Reflections occurs from planes set at angle Θ with respect to the incident beam and generates a reflected beam at an angle 2Θ from the incident beam. The possible d-spacing defined by the indices h, k, l are determined by the shape of the unit cell. Rewriting

Bragg's law we get:

$$\sin T = A / 2d$$

Therefore the possible 2Θ values where we can have reflections are determined by the unit cell dimensions. However, the intensities of the reflections are determined by the distribution of the electrons in the unit cell. The highest electron density is found around atoms. Therefore, the intensities depend on what kind of atoms we have and where in the unit cell they are located. Planes going through areas with high electron density will reflect strongly, planes with low electron density will give weak intensities.

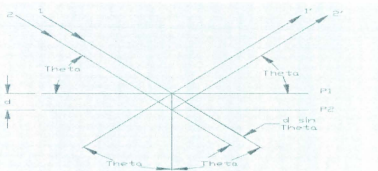


Figure 2.6: Schematic diagram of XRD theory.

2.5.4 Chemical Analysis by SEM

A scanning electron microscope (SEM) is a type of electron microscope that images a sample by scanning it with a beam of electrons in a raster scan pattern. The electrons interact with the atoms that make up the sample producing signals that contain information about the sample's surface topography, composition, and other properties such as electrical conductivity.

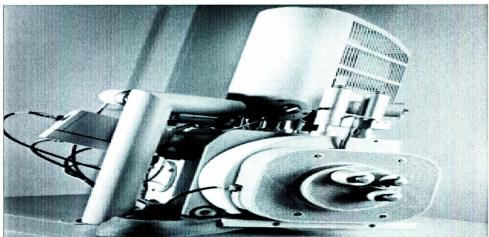


Figure 2.7: FEI Quanta 400 environmental SEM. (SEM, 2012)

A wide range of magnifications is possible, from about 10 times (about equivalent to that of a powerful hand-lens) to more than 500,000 times, about 250 times the magnification limit of the best light microscopes. Back-scattered electrons (BSE) are beam electrons that are reflected from the sample by elastic scattering. BSE are often used in analytical SEM along with the spectra made from the characteristic X-rays. Because the intensity of the BSE signal is strongly related to the atomic number (Z) of the specimen, BSE images can provide information about the distribution of different elements in the sample. For the same reason, BSE imaging can image

colloidal gold immuno-labels of 5 or 10 nm diameters, which would otherwise be difficult or impossible to detect in secondary electron images in biological specimens. Characteristic X-rays are emitted when the electron beam removes an inner shell electron from the sample, causing a higher-energy electron to fill the shell and release energy. These characteristic X-rays are used to identify the composition and measure the abundance of elements in the sample.

2.5.4.1 Scanning process and image formation

In a typical SEM, an electron beam is thermionically emitted from an electron gun fitted with a tungsten filament cathode. Tungsten is normally used in thermionic electron guns because it has the highest melting point and lowest vapour pressure of all metals, thereby allowing it to be heated for electron emission, and because of its low cost. Other types of electron emitters include lanthanum hexaboride cathodes, which can be used in a standard tungsten filament SEM if the vacuum system is upgraded and field emission guns (FEG), which may be of the cold-cathode type using tungsten single crystal emitters or the thermally assisted Schottky type, using emitters of zirconium oxide.

The electron beam, which typically has an energy ranging from 0.2 keV to 40 keV, is focused by one or two condenser lenses to a spot about 0.4 nm to 5 nm in diameter. The beam passes through pairs of scanning coils or pairs of deflector plates in the electron column, typically in the final lens, which deflect the beam in the x and y axes so that it scans in a raster fashion over a rectangular area of the sample surface.

2.5.4.2 Magnification

Magnification in a SEM can be controlled over a range of up to 6 orders of magnitude from about 10 to 500,000 times. Unlike optical and transmission electron microscopes, image magnification in the SEM is not a function of the power of the objective lens. SEMs may have condenser and objective lenses, but their function is to focus the beam to a spot, and not to image the specimen. Provided the electron gun can generate a beam with sufficiently small diameter, a SEM could in principle work entirely without condenser or objective lenses, although it might not be very versatile or achieve very high resolution. In a SEM, as in scanning probe microscopy, magnification results from the ratio of the dimensions of the raster on the specimen and the raster on the display device. Assuming that the display screen has a fixed size, higher magnification results from reducing the size of the raster on the specimen, and vice versa. Magnification is therefore controlled by the current supplied to the x, y scanning coils, or the voltage supplied to the x, y deflector plates, and not by objective lens power.

2.5.4.3 Sample preparation

All samples must also be of an appropriate size to fit in the specimen chamber and are generally mounted rigidly on a specimen holder called a specimen stub. Several models of SEM can examine any part of a 6-inch (15 cm) semiconductor wafer, and some can tilt an object of that size to 45°.

For conventional imaging in the SEM, specimens must be electrically conductive, at least at the surface, and electrically grounded to prevent the accumulation of electrostatic charge at the surface. Metal objects require little special preparation for SEM except for cleaning and mounting on a specimen stub. Nonconductive specimens tend to charge when scanned by the

electron beam, and especially in secondary electron imaging mode, this causes scanning faults and other image artifacts. They are therefore usually coated with an ultrathin coating of electrically conducting material, deposited on the sample either by low-vacuum sputter coating or by high-vacuum evaporation. Conductive materials in current use for specimen coating include gold, gold/palladium alloy, platinum, osmium, (5) iridium, tungsten, chromium, and graphite. Additionally, coating may increase signal/noise ratio for samples of low atomic number (Z). The improvement arises because secondary electron emission for high-Z materials is enhanced.

CHAPTER 3

3 Materials and Methods

3.1 Preparation of Metal Ion Solutions/Chemicals and Analysis

All chemicals used in this research were of analytical grade and used without further purification. Aqueous Metal solutions were prepared by dissolving corresponding analytical grade Lead(II) chloride, zinc(II) sulphate and copper(II) sulphate in dilute sulphuric acid solution (18 M) and sodium hydroxide solution (1 M), which were mixed in arbitrary volume to adjust pH to provide test solutions of corresponding single metal ions. Also Sample solution taken from the Buchans mine are also used for testing.

3.2 Preparations of the Adsorption Gel from Orange Juice Residue

Orange waste principally consists of cellulose, hemicellulose, pectin, chlorophyll pigment and other low molecular weight compounds like limonene and so on. Pectin contains carboxyl groups as well as its methyl ester groups. The methyl ester portion of orange pectin can be easily converted into carboxyl group by saponification reaction with lime water as follows. At first, 100 g of orange waste was washed several times with distilled water to remove water soluble organic compounds that could hinder the saponification reaction. Thus, pretreated orange waste was then mixed together with 8 g of calcium hydroxide and was grounded into fine particles with the help of BLENDERPRO HL-2170-2 grinder. The reaction mixture was shaken at a INNOVA 43 Incubator for 24 h at 30 °C after the addition of substantial amount of water to enhance the saponification of methyl ester portion of pectin in orange waste by lime water according to the reaction described by Figure 3.1.

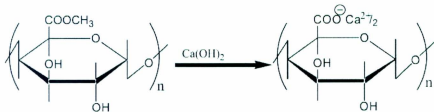


Figure 3.1: Synthetic route of SOJR

The initial pH of the reaction mixture was adjusted at around 12 by adding sodium hydroxide pellets. After the saponification, the suspension was washed with distilled water via decantation, which was followed by filtration until neutral pH, and finally the residual product was dried in a convection oven at 70 °C. The white product prepared in this way contains calcium salt of pectic acid and was termed as saponified orange juice residue, abbreviated as SOJR hereafter. The product was grounded by mortar and sieved to obtain the particle size of 100-150 µm gel.

3.3 Analysis

The pH and concentration of metal solution were measured by using ORION 5STAR series pH meter, calibrated with buffers of pH 2.0, 4.0, 7.0 and 10.0 on a regular basis and a Perkin Elmer Optima Inductive Couple Plasma optical Emission spectrometer (ICPOES), respectively.

The characterization of the Adsorbents before and after adsorption was done by Rigaku Ultima IV X-ray diffractometer with a copper X-ray source and a scintillation counter detector, Bruker TENSOR 27 infrared spectrometer and FEI Quanta 400 environmental Scanning Electron Microscope. Reproducibility of all adsorption experiments was confirmed by repeating the same adsorption test.

3.4 Batch Wise Adsorption Tests

All adsorption tests of metal ions were carried out by the conventional batch method using aqueous test solutions containing metal ions. In the batch wise adsorption studies, 20 mg (dry weight) of adsorption gel was shaken vigorously with 20 cm³ test solution in a 50 cm³ conical flask in a thermo stated shaker maintained at 30°C for 24 h at 300 rpm to maintain equilibrium. After which the suspended mixture was filtered and residual concentrations in the filtrate were

measured. The initial concentration was also measured along with this for the accuracy. The effect of concentration on metal adsorption was examined at different concentration between 10 ppm to 100 ppm at initial pH of 3.5. The effect of pH on metal adsorption was examined at different pH (1 to 7) at 1 mM metal concentration. The effect of solid liquid ratio on metal adsorption was examined at different solid/liquid ratio (1 to 3). Isotherm studies were conducted by varying the initial metal concentration (10 ppm-100 ppm) at pH 3.5.

The amount of metal adsorption ($q/\text{mol kg}^{-1}$) was calculated according to Eq. (3.1) from the metal concentrations before and after the adsorption (C_0 and C_e / M , respectively), the dry weight of the adsorption gel (W/kg), and the volume of aqueous solution (V/dm^3).

The percentage adsorption ($R/\%$), defined as the ratio of decrease in metal concentration in aqueous solution before and after adsorption ($C_o - C_e$) to its initial concentration (C_o), was calculated according to Eq. (3.2).

3.5 Kinetic Studies

For the kinetic studies, 20 mg of SOJR was taken in a 50 cm³ conical flask together with 20 cm³ sample solution of two different pH. The flasks were then shaken at constant temperature 30°C at the speed of 300 rpm. Samples were taken at predetermined time intervals (6-8 different times). After that, the samples were filtered immediately through filter paper and the filtrate was analyzed to determine the concentration of metal remaining in the filtrate.

3.6 Isotherm and Kinetic Models

Langmuir model is presented by Eq. (3.3);

where q_e and q_m are the equilibrium and maximum metal adsorption of metal ion per unit weight of adsorbent to form a complete monolayer on the surface bound at C_e ; respectively; b is the equilibrium constant.

Freundlich model is given by Eq. (3.4);

Where K^f and n are the Freundlich constants, which features the system, respectively.

Pseudo-first-order kinetic model (Cheung et al., 2001; Bayramoglu et al. 2002) was generally expressed as Eq. (3.5):

$$\ln \left(\frac{q_e - q_t}{q_t} \right) = -K_1 t. \dots \quad (3.5)$$

Where q_t is the amount of the metal ions adsorbed (mol/kg) at time t (min), q_e is the amount of metal at equilibrium (mol/kg) and K_1 is the adsorption rate constant of the pseudo-first-order equation (l/min).

Pseudo-second-order kinetic model (Ho and McKay, 1999) was expressed by Eq. (3.6):

Where q_t is the amount of the metal ions adsorbed (mol/kg) at time t (min), q_e is the amount of metal at equilibrium (mol/kg) and K_2 is the adsorption rate constant of the pseudo-second-order equation (l/min).

3.7 XRD Analysis

XRD analysis was performed on Rigaku Ultima IV X-ray diffractometer with a copper X-ray source. The Ultima IV, with Rigaku's patented Cross Beam Optics (CBO), is a flexible, multi-purpose XRD. It incorporates fully automatic alignment and allows for fast, easy switching between focusing and parallel beam geometries without the need to reconfigure the system. Other features of the Ultima IV at Memorial University are the automatic 10-position sample changer with spinner and the high temperature (1500 °C) attachment. The experiments were carried out at The Earth Resources Research and Analysis (TERRA) Facility, Memorial University of Newfoundland.

3.8 FT-IR Analysis

FT-IR analysis was performed on Bruker TENSOR 27 infrared spectrometer. This instrument has a spectral range of 7,500 to 370 wave numbers and is equipped with a Miracle ATR accessory allowing rapid and easy analysis of liquid and solid samples. The experiments were carried out at the Centre of Chemical Analysis, Research and Training (C-CART) at Memorial University of Newfoundland.

3.9 Scanning Electron Microscope (SEM) Analysis

Scanning Electron Microscope Analysis was performed on FEI Quanta 400 environmental SEM. The term environmental refers to this SEM's capability for working at near atmospheric pressures instead of high vacuum. This capability allows for almost any specimen to be examined, including wet and non-conducting specimens.

For accommodating the variety of information available from electron interaction, SEM is also equipped with an energy dispersive X-ray (EDX) analytical system from Roentec. The experiments were carried out at Micro Analysis Facility-INCO Innovation Centre (MAF-IIC), Memorial University of Newfoundland.

CHAPTER 4

4 Results and Discussions

4.1 Characterization of the Adsorbent

Peel, pulp and membranes from oranges are highly susceptible to hydrolysis by mixture of cellulosic and pectinolytic enzymes (Grohmann and Baldwin, 1992). It is a pectin rich biopolymer that can be chemically modified by lime water to SOJR, which can act like an anion exchanger when it is loaded with metal ions.

4.2 Adsorptive Removal of Metal Ions

Table 4.1 shows amount of adsorption ($q/\text{mol kg}^{-1}$) and percentage of adsorption (R) of different metal ions in different acid mine drainage sample by Ca^{2+} -form SOJR. Five different sample were tested with same pH and solid liquid ratio but at different concentrations.

Table 4.1: Amount of adsorption ($q/\text{mol kg}^{-1}$) and percentage of adsorption (R) of different metal ions in different water sample by Ca^{2+} -form SOJR. Solid/Liquid ratio=1, Weight of the gel = 20 mg. Volume of the aqueous solution= 20 mL.

Sample	Amount of adsorption, $q(\text{mol/kg})$			Percentage of Adsorption, R (%)		
	Cu	Zn	Pb	Cu	Zn	Pb
Background water	0.08	0.01	0.02	66.84	1.90	97.44
Upstream pond	0.11	0.07	0.02	46.40	20.52	91.95
Diversion Ditch	0.32	0.13	0.02	42.59	18.98	86.70
Pipe samples 1	0.44	0.09	0.19	35.47	8.28	97.06
Pipe samples 2	0.44	0.13	0.25	29.91	9.07	96.98

Figure 4.1 shows the effect of concentration on the adsorption of various metal ions by the SOJR at an initial pH 3.5. Adsorption behavior is almost same in the case of Pb(II) and Zn(II), but it decreases in case of Cu(II). The selectivity order for various metal ions tested is as follows: Pb(II)>Cu(II)>Zn(II).

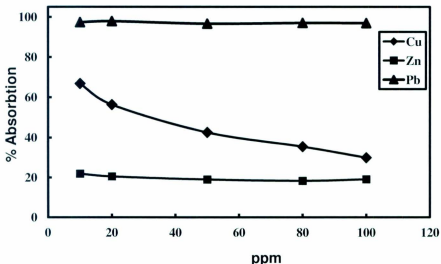
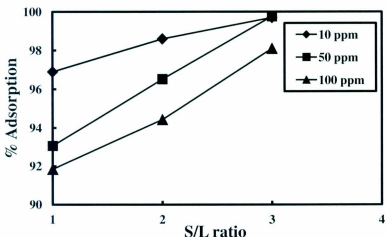


Figure 4.1: Removal of metal ions from aqueous solution on the Ca^{2+} -form SOJR as a function of initial concentration. Weight of the gel= 20 mg. Initial pH= 3.5. Volume of the aqueous solution= 20 mL.

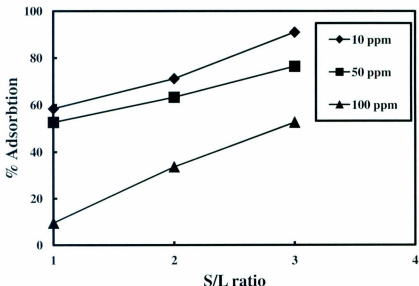
4.3 Effect of Solid/Liquid Ratio on Metal adsorption

Figures 4.2 (a), (b) and (c) show the effect of solid liquid ratio on the adsorptive removal of the Lead(Pb), Copper(Cu), and Zinc(Zn) respectively by the SOJR with different concentration of metal ions of (10, 50 and 100 ppm) at the initial pH of 3.5. Adsorption increases with the increases of solid liquid ratio. However like Fig. 4.1 for Pb (II), it does not change for different concentration, where as in the case of Zn(II) and Cu(II) it increases with the increase of concentration, which clearly indicate the saturation of adsorbent. The selectivity order is Pb (II)>Cu (II)>Zn (II).



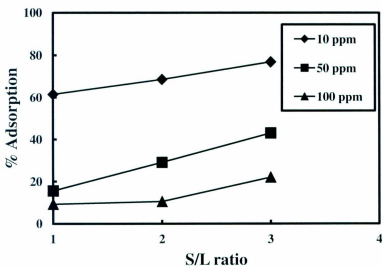
(a)

Figure 4.2(a): Removal of Lead (Pb) ions from aqueous solution on the Ca^{2+} -form SOJR as a function of solid/liquid ratio. Weight of the gel= 20, 40, 60 mg. Initial pH= 3.5. Volume of the aqueous solution= 20 mL. Initial concentration= 10, 50 and 100 ppm.



(b)

Figure 4.2(b): Removal of Copper(Cu) ions from aqueous solution on the Ca^{2+} -form SOJR as a function of solid/liquid ratio. Weight of the gel = 20, 40, 60 mg. Initial pH = 3.5. Volume of the aqueous solution = 20 mL. Initial concentration = 10, 50 and 100 ppm.



(c)

Figure 4.2(c): Removal of (Zn) ions from aqueous solution on the Ca^{2+} -form SOJR as a function of solid/liquid ratio. Weight of the gel= 20, 40, 60 mg. Initial pH= 3.5. Volume of the aqueous solution= 20 mL. Initial concentration= 10, 50 and 100 ppm.

4.4 Influence of pH for the Metal Adsorption

Figure 4.3 shows the effect of equilibrium pH on the adsorption of various metal ions by SOJR at an initial concentration of 1 mM. Adsorption increases with increasing pH in the case of Zn(II). In the case of Pb(II) it slightly change. In the case of Cu(II) it increases with the increasing of pH. The result shows that optimum adsorption for metals have taken place in the pH region of 3 to 5. The pH decreased after adsorption in all cases, this suggests that uptake of metal ions takes place according to an ion exchange mechanism. The selectivity order for various metal ions tested are as follows: Pb(II)>Cu(II)>Zn(II).

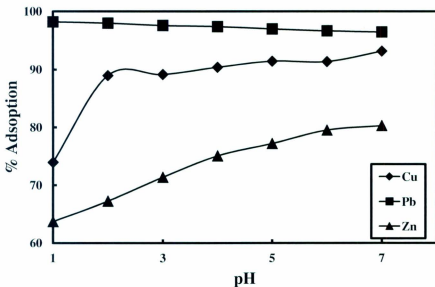


Figure 4.3: Removal of metal ions from aqueous solution on the Ca^{2+} -form SOJR as a function of equilibrium pH. Weight of the gel= 20 mg. Volume of the aqueous solution= 20 mL. Initial metal concentration= 1mM.

4.5 Adsorption Isotherms

Figure 4.4 shows the experimental isotherms obtained for metals binding. It shows that the adsorption capacity increased with increasing equilibrium concentration of metal, progressively reaching saturation of the adsorbent. The Langmuir, Freundlich and Langmuir-Freundlich (L-F) isotherm models were then applied to the experimental data and the obtained parameters are presented in Table 4.2. The initial isotherm gradient indicates the sorbent affinity at low metal concentrations. In the Langmuir equation, this initial gradient corresponds to the affinity constant b . Davis et al. (2003) and Murphy et al. 2008 showed that high b values reflect high affinity of the sorbent for the metal. From Fig. 4.4 and Table 4.2 it is clear that most of the bioadsorbents have a high b value and are suitable for metal binding. They also possess a comparatively large q_m .

According to the data given in Table 4.2, a comparison of different isotherm models with the correlation coefficients R^2 revealed that a pseudo-second-order isotherm models fitted the experimental data best. The q_m values obtained from the pseudo-second-order isotherm for metal binding decreased in the order of Cu(II)>Pb(II)>Zn(II). The maximum uptake of metal ions achieved are 0.95, 0.63 and 0.295 mol/kg for Cu(II), Pb(II), Zn(II), respectively.

Table 4.2: Pseudo-first-order, pseudo-second-order, Langmuir, Freundlich model parameters for metal bioadsorption equilibrium on Ca^{2+} -form SOJR.

Metal type	Pseudo-first-order			Pseudo-second-order			Lang muir	Freundl ch	R^2	
	qe(mol/kg)	K1 (1/min)	R^2	qe(mol/kg)	K2(kg/mol min)	R^2				
Cu(1)	0.250095	0.03493 2	0.86 08	0.25009 5	0.18366333 1	0.9954	200 7	0.96 0.025	2.1 6	0.9 1
Zn(1)	0.817968	0.00582 8	0.95 83	0.81796 8	0.00744595 8	0.8387	0.236 84	0.53 0.0023	0.2 5	0.8
Pb(1)	0.129381	0.00926 3	0.75 3	0.12938 1	0.07680430 6	0.9318	127.1 89	0.75 0.0007	0.9 8	0.7 8
Cu(2)	0.100069	0.01695 5	0.78 77	0.10006 9	0.19306588 6	0.9809	648.1 7	0.79 0.012	4.1 6	0.8 3
Zn(2)	0.942622	0.01622 3	0.97 03	0.94262 2	0.01948529 3	0.9808	4.33 7	0.87 0.012	0.3 1	0.9 4
Pb(2)	0.107082	0.06417 3	0.77 72	0.10708 2	0.38481559 1	0.997	413.3 5	0.97 76	0.011 0.011	0.9 2.4

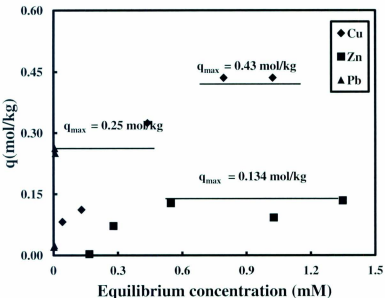
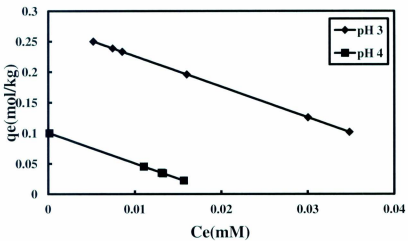
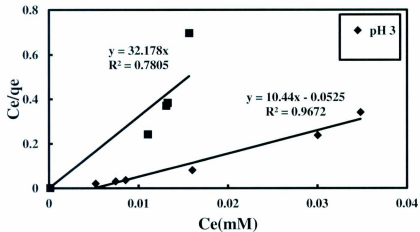


Figure 4.4: Adsorption isotherms of some metal ions at pH 3.5. Volume of the aqueous solution = 20 mL. Weight of the gel= 20 mg.

Figure 4.5(a,b), 4.6(a,b), 4.7(a,b) presents the adsorption isotherms of three metal ions at various pH values. The adsorption capacity increased with decreasing equilibrium concentration of metal. All the adsorption isotherms in Figure 4.5 fitted to the Langmuir model with high correlation coefficients ($R^2 > 0.95$). The q_m values at pH 3 and 4 were also calculated using the Langmuir model.

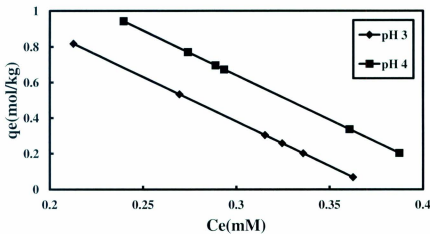


(a)

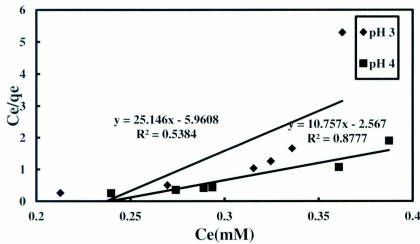


(b)

Figure 4.5: (a) Adsorption isotherms at different pH and (b) corresponding Langmuir Plots for Cu(II).

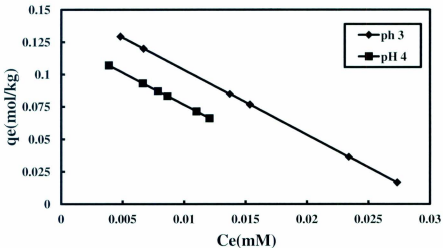


(a)

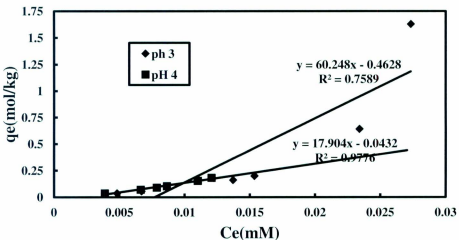


(b)

Figure 4.6: (a) Adsorption isotherms at different pH and (b) corresponding Langmuir Plots for Zn(II).



(a)



(b)

Figure 4.7: (a) Adsorption isotherms at different pH and (b) corresponding Langmuir Plots for Pb(II).

4.6 Kinetic Studies

Figure 4.8 illustrates the evolution of metal uptake with time for two different types of acid mine drainage samples. Adsorption occurs mainly within the first 240 min. Faster kinetics has significant practical importance as it will facilitate the scale up of the process to small reactor volumes, ensuring efficiency and economy. This behaviour is typical of biosorption of metals involving purely weak intermolecular forces between the biomass and the metal in solution.

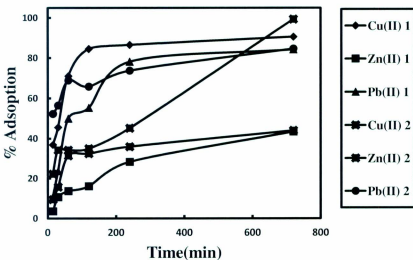


Figure 4.8: Adsorption kinetics at different acid mine sample of different AMD sample.

4.7 Proposed Mechanism of Metal Adsorption

It is evident from the research results that heavy metal like Pb, Cu and Zn were strongly adsorbed on SOJR at pH 3-5, whereas it was poorly adsorbed at alkaline pH, suggesting the possibility of elution of metal using alkaline solution, from which it is suggested that the adsorption mechanism of metal on SOJR is interpreted as follows. The adsorption of metal cations takes place according to a cation exchange mechanism releasing calcium ions (Ca^{2+}) from the carboxylic groups of pectic acid as shown in Fig. 4.9.

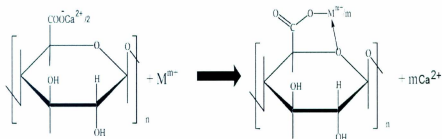


Figure 4.9: Adsorption mechanism of metal cations on pectin.

4.8 XRD Analysis Result

XRD is a bulk method, and reveals information on the bulk structure of the catalyst and its support.

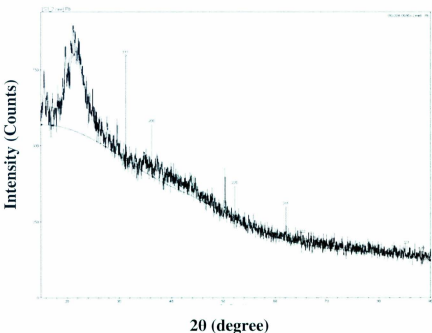


Figure 4.10: XRD pattern of a SOJR containing Pb.

The first peak, at the low 2θ range, is associated with the carbon support. Figure 4.10 shows the XRD pattern of SOJR supported pure lead following thermal treatment up to 400 °C. The Pb pattern displayed the [111], [200], [220] and [311] reflexions characteristic of f.c.c. crystal structure. XRD patterns of the samples thermal treated at temperatures lower than 300 °C displayed the reflexions of the carbon only. This indicates the presence of small and poor

crystalline metal particles, with a weak internal organization. Starting from thermal treatment at 300 °C, the patterns displayed the reflexions characteristic of lead f.c.c. crystal structure, with some shift in the position of each reflexion peak. The shifts in 2θ correspond to decreased lattice constant due to incorporation of Pb atoms. The f.c.c. reflexions showed a tail, which can be attributed to a low composition homogeneity. Pb particle size, calculated from the XRD patterns using the Scherrer formula, was in the range 15–20 nm.

4.9 FT-IR Analysis Result

IR analysis permits spectrophotometric observation of the adsorbent surface in the range of 400–4000 cm^{-1} and serves as a direct means for the identification of functional groups on the surface. An examination of the adsorbent before and after sorption reaction possibly provides information regarding the surface groups that might have participated in the adsorption reaction and also indicates the surface sites on which adsorption have taken place. However, FT-IR spectra of the SOJR before and after heavy metal (Pb, Cu, Zn) adsorption were taken (Figs. 4.11 and 4.12) in order to understand the structural change as well as the involvement of main functional groups in arsenic adsorption. Since the structure of the gel is complex, a complete diagnosis of the spectra seems to be difficult to elucidate. An attempt, however, has been made to explain the structural changes during the adsorption of arsenic.

Both spectra show the O-H stretching region at around 3400 cm^{-1} . Carboxyl group is supposed to be a characteristic group of pectic acid, which is the key compound found in orange waste for making adsorption gel.

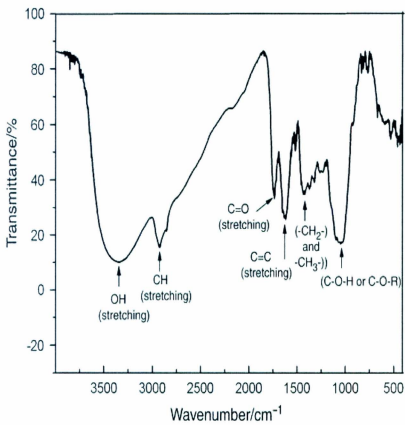


Figure 4.11: FT-IR Analysis of the SOJR.

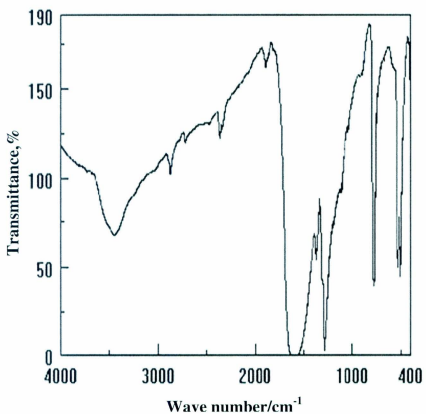


Figure 4.12: FT-IR Spectrum of SOJR after metal adsorption.

4.10 Scanning Electron Microscope (SEM) Analysis

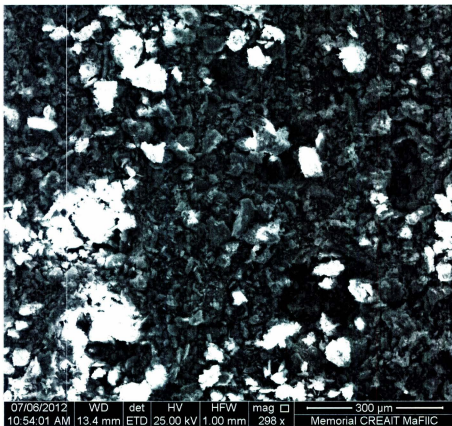
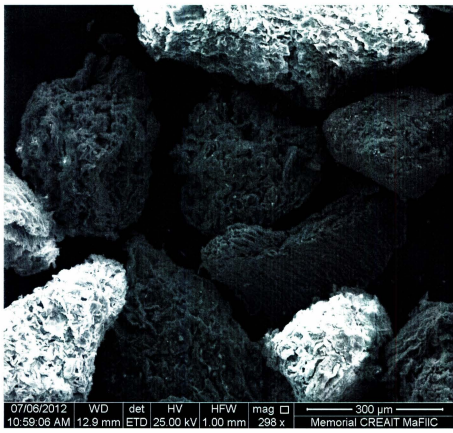


Figure 4.13: SEM photograph of SOJR.



07/06/2012	WD	det	HV	HFW	mag	□	300 μm
10:59:06 AM	12.9 mm	ETD	25.00 kV	1.00 mm	298 x		Memorial CREAT MaFiC

Figure 4.14: SEM photograph of SOJR after metal adsorption.

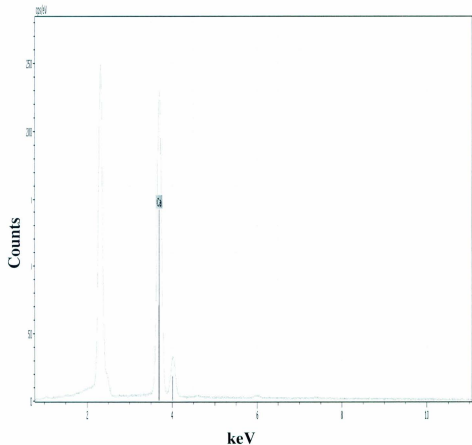


Figure 4.15: EDX analysis of Ca^{2+} -form SOJR by SEM.

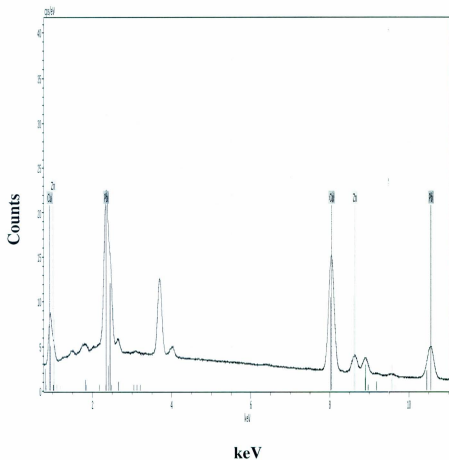


Figure 4.16: EDX analysis of Ca^{2+} -form SOJR with metals by SEM

The electron microscopy (SEM) images presented in Fig. 14.13 reveal randomly distributed pore structures for SOJR. Evidence of large internal surface areas in the microporous structures within the SOJR is presented in this Figure. The SEM image in Fig. 4.14 presents SOJR after metal adsorption and the presence of numerous inner micropores. From this image, it can be seen that there is a highly microporous structures in SOJR, which can provide the maximum number of possible metal loading sites.

The EDX analysis graphs presented in Figs. 4.15 and 4.16 clearly show the presence of metal in SOJR only after adsorption. Figure 4.16 presents the highly capability of SOJR for lead adsorption.

4.11 Research Findings

In this work, we investigated the Saponified orange gel residue as an adsorbent to remove heavy metals from waste solution. As a waste we used the Acid Mine Drainage water, which has a big environmental concern for its high heavy metal concentration. Orange peel is a pectin rich bio-polymer that can be chemically modified by lime water to SOJR which can act like an anion exchanger when it is loaded with metal ions. The results of the adsorption experiments suggest that SOJR can be applied for wastewater treatment as an immobilizer of pollutants. The results found that SOJR was effective in reducing the Pb, Cu, and Zn concentration, with the complete removal of Pb from AMD. The concept of SOJR is not unique, but using it as an adsorbent to uptake heavy metal from acid mine waste is a new thing. Orange waste cellulose was chosen as

biosorbent due to its special structure, insolubility in water, chemical stability and local availability. The core findings of this research are:

- Lead was almost completely removed from acid mine drainage solution by saponified orange Juice residue (SOJR).
- The effective pH range was found to be 3 to 5.
- Copper and Zinc were also removed to create a tolerable limit from acid mine drainage.
- The maximum loading capacities for Pb (II), Cu (II) and Zn (II) were found to be 0.25, 0.43 and 0.134 mol/kg, respectively.
- The heavy metal removal was effected by on the pH, sorbent dosage and initial concentrations.
- The adsorption capacity was increased with increasing equilibrium concentration of metal.
- The adsorption of metal cations took place according to a cation exchange mechanism releasing calcium ions from the carboxilic groups of pectic acid.

CHAPTER 5

5 Conclusion and Recommendation

5.1 Conclusion

In this study Saponified Orange Juice Residue was investigated in batch experiments as potential adsorbents for the treatment of AMD. There are two competing processes here, the release of alkalinity from adsorbents and the removal of acidity from AMD components. At higher adsorbent dosage the acidity from AMD components is overwhelmed and the pH is bound to increase, while with lower sorbent dosage the alkalinity from the sorbent is overwhelmed by the acidity from the AMD components and the pH remains low. The experimental data shows that the heavy metal removal depends on the pH, sorbent dosage and initial concentrations. The kinetic study at different metal concentrations and pH values are well described by the pseudo-first and second- order model as well as the Langmuir and Freundlich model. The results of the adsorption experiments suggest that SOJR can be applied for wastewater treatment as an immobilizer of pollutants. From the above results, we have shown that SOJR was effective in reducing the Pb, Cu, and Zn concentration, indicating the complete removal of Pb. Our result can be applied in waste management areas, especially in AMD treatment. It will be necessary to design and execute some more detailed experiments to explore further application of the SOJR for cleanup of the AMD. This can be treated at the mine to some degree, usually by

neutralisation at source by rocks, settling and tailings ponds or wetlands, although this process may not be fully efficient with the treatment system are inevitable.

5.2 Recommendation for Future Work

In the research, all experiments were conducted batch wise. But for effectiveness in wastewater treatment it will be necessary to do the tests by continuous column method. For the AMD treatment a sustainable process flow should be done for maximum utilisation of this environment friendly bioadsorbent. A mine-drainage treatment facility must have the flexibility to deal with increasing/decreasing water flows, changing water qualities and regulatory requirements over the life of mine. This may dictate phased implementation and modular design and construction. Additionally, the post-closure phase may place specific constraints on the continued operation and maintenance of a treatment facility.

PART 2

Recovery of Gold from Synthetic Solution using Cellulose Base

Bioadsorbent from Paper and Cloth

CHAPTER 6

6 Introduction

6.1 Background

Gold is the most versatile metal which possesses many unique properties. Apart from various traditional uses, its application in many technical purposes is now increasing. Nowadays, gold is widely used in various industries, agriculture and medicine, because of its specific physical and chemical properties (Ramesh et al., 2008). The use of gold in industrial applications has recently become extensive, e.g., electrical systems and devices, fuel cells, catalysts, biomedical area, etc. (Corti and Holliday, 2004). Economically, gold is historically important as currency, and remains important as investment commodities. Gold (Au), silver (Ag), platinum (Pt) and palladium (Pd) are internationally recognized as forms of currency under ISO 4217.

Because of the limited availability of gold, recovery of these metals from aqueous and waste solutions is economically attractive. Millions of tons of spent electrical and electronic devices are discarded every year. More than half of these wastes consist of metals including a significant proportion of valuable metals or their compounds, which indicates not only the loss of huge amounts of resources but also the threat of environmental pollution. The high pace of technological change and competitive market strategies that encourage people to buy the latest models before their old appliances stop functioning have caused an alarming increase in electronic and electrical wastes. Along with other useful valuable metals, gold, which is mainly used in making gold-coated edge contacts on printed circuit boards, is also being wasted. In a rough estimate, the percentage composition of different metals by weight in a mobile phone, for

example, is as follows: copper, 15%; iron, 3%; zinc, 1%; and less than 1% of a number of metals such as tin, palladium, and gold (Ramesh et al., 2008). Although the portion of gold is very low compared to the other metals in one piece of a device, the amount of gold disposed in this form is much higher than the content in gold ore itself (Corti and Holliday., 2004).

The demand for gold (Au) has been increasing since it is used as a monetary standard and its wide utilization in different applications. The increased demand for gold has increased interest in the recovery of gold from waste solutions such as those from refining or mining effluents with high concentrations of gold. For a sustainable society and strong economy, it becomes necessary to recycle and reuse such precious metal resources in order not to waste them. Industrial cycling techniques such as pyrometallurgical and hydrometallurgical processes have been widely used to recover gold from wastes (Jacobsen, 2005).

The increase in the industrial demand for gold will correspond to the increase in the need for gold recycling. In general, gold is separated and purified from industrial wastes by hydrometallurgical processes involving chloride media (Iglesias, 1999). The hydrometallurgical methods, which includes adsorption by ion exchange resin, solvent extraction, and the reduction of precious metal precipitate by reagents, has been utilized more often than the pyrometallurgical process. Both of these recovery methods are costly and require extensive labor and time. Furthermore, large quantities of secondary waste are generated resulting from the addition of chemical agents for precipitation and reduction in the processes. Therefore, there is a need to develop a system to recover gold from waste e.g. low cost and eco-friendly.

Bioadsorption is considered a promising technology for the recovery of gold. This is due to the fact that the properties of certain types of inactive or dead microbial biomass materials allow

them to bind and concentrate metal ions from industrial effluents and aqueous solutions (Dobson and Burgess, 2007). These types of biomasses are relatively inexpensive and available in large quantities. Bioadsorption is a metabolism independent process that takes place in the cell wall (Mao et al., 2009), and the mechanism responsible for the metal uptake may differ according to the biomass type.

Cost effectiveness is the main attraction of metal bioadsorption. Since bioadsorption often employs dead biomass, this eliminates the need of nutrient requirement and can be exposed to environments of high toxicity (Volesky, 1990). A major advantage of bioadsorption is that it can be used *in situ*, and with proper design may not need any industrial process operations and can be integrated with many systems in the most eco-friendly manner (Tewari et al., 2005).

In recent years, a variety of adsorbents prepared from biomass wastes and natural products including tannin, algae, fungi and yeast biomass, alfalfa, various protein sources and fruit wastes [(Ogata and Nakano, 2005), (Gomes et al., 2001), (Pethkar and Paknikar, 1998), (Kiyoyama et al., 2008), (Karamuchka and Gadd, 1999), and (Abidin et al. 2011)], have been tested for the recovery of gold. However, naturally abundant and low cost adsorption materials are still required to recover gold, particularly from wastewater from electronic and electroplating factories and leach liquor of e-wastes.

Cellulose constitutes the most abundant and renewable polymer resource available worldwide. It is estimated that by photosynthesis, 10^{11} – 10^{12} tons of cellulose are synthesized annually in a relatively pure form, for example, in the seed hairs of the cotton plant, but more often are combined with lignin and other polysaccharides in the cell wall of woody plants (Klemm et al.,

2002). Cellulose has been used in the form of wood and cotton for thousands of years as an energy source, a building material and for clothing.

The molecular structure of cellulose as a carbohydrate polymer is comprised of repeating β -d-glucopyranose units which are covalently linked through acetyl functions between the OH group of the C₄ and C₁ carbon atoms (β -1, 4-glucan). Cellulose is a large, linear-chain polymer with a large number of hydroxyl groups (three per anhydroglucose (AGU) unit) and present in the preferred 4C_1 conformation. To accommodate the preferred bond angles, every second AGU unit is rotated 180° in the plane. The length of the polymeric cellulose chain depends on the number of constituent AGU units (degree of polymerisation, DP) and varies with the origin and treatment of the cellulose raw material (Klemm et al., 2002).

In particular, two main approaches have been attempted in the conversion of cellulose into compounds capable of adsorbing heavy metal ions from aqueous solutions. The first of these methods involves a direct modification of the cellulose backbone with the introduction of chelating or metal binding functionalities producing a range of heavy metal adsorbents. Alternative approaches have focused on the grafting of selected monomers to the cellulose backbone, either directly introducing metal binding capability or with subsequent functionalisation of these grafted polymer chains with known chelating moieties.

Unmodified cellulose has a low heavy metal adsorption capacity as well as variable physical stability. Therefore, chemical modification of cellulose can be carried out to achieve adequate structural durability and an efficient adsorption capacity for heavy metal ions (Kamel et al., 2006). Chemical modification can be used to vary certain properties of cellulose such as its

hydrophilic or hydrophobic character, elasticity, water sorbency, adsorptive or ion exchange capability, resistance to microbiological attack and thermal resistance (McDoall et al., 1984).

The dosage of a bioadsorbent strongly influences the extent of bioadsorption. An increase in the biomass concentration generally increases the amount of solute bioadsorbed due to increased surface area of the biosorbent which in turn increases the number of binding sites (Esposito et al. 2001). On the other hand, the quantity of bioadsorbed solute per unit weight of bioadsorbent decreases with increasing bioadsorbent dosage which may be due to the complex interaction of several factors. An important factor at high sorbent dosages is that the available solute is insufficient to completely cover the available exchangeable sites on the bioadsorbent, usually resulting in low solute uptake (Tangaromsuk et al., 2002). Also, as suggested by Gadd (Gadd et al., 1988) the interference between binding sites due to increased bioadsorbent dosages cannot be overruled, as this will result in a low specific uptake.

6.2 Objective of the Research Work

In this project, investigations were carried out; starting from the preparation of cellulose based bioadsorbent using waste cloth and shredded paper in a very simple way and using a very low amount of chemicals. Experiments were done to observe the capacity, selectivity of the gels on gold or other precious metals adsorption. The factors which can affect the reaction by percentage, time or selectivity were also investigated. Kinetic studies of the reaction were observed by plotting different equations to try and find a good and acceptable result for both pilot and industrial scale. XRD and FT-IR analysis were conducted for confirmation of the

adsorption. SEM analysis was done to see the molecular bonding structure of gold by the adsorbent.

6.3 Organization of this part of the thesis

This part of the thesis has been organized as follows:

Chapter 6 provides the key research introduction and objectives followed by the organization of thesis.

Chapter 7 provides a detailed literature review. The literature review starts with a broad point of view like precious metals and recovery of precious metals and has been narrowed down to gold adsorption and with elaborate description of cellulose based bioadsorbents, like paper and cotton.

Chapter 8 describes the detailed experimental studies performed in this research with a brief description of the adsorbents.

Chapter 9 is the most important part of this thesis, which describes the research findings and presents an elaborate discussion with comparison of the results of this study.

Chapter 10 describes the research conclusion along with the future recommendations to continue this research.

CHAPTER 7

7 Literature Review

7.1 Precious Metals and Recovery of Precious Metals

7.1.1 Precious Metals

Precious metals are rare, naturally occurring metallic chemical elements that have high economic value. They are less reactive than most elements. They are usually ductile and have a high lustre. Precious metals were important as currency but are now regarded mainly as investment and industrial commodities. The best-known precious metals are the coinage metals gold and silver. They both have industrial uses and they are better known for their uses in art, jewellery and coinage. Other precious metals include the platinum group metals: ruthenium, rhodium, palladium, osmium, iridium, and platinum (Precious Metal, 2012).

Due to the limited availability of precious metals, recovery of these metals from aqueous and waste solutions is economically attractive. Pyrometallurgical and hydrometallurgical processes have been widely used to recover precious metals (Jacobsen, 2005). Adsorption by ion exchange resin, solvent extraction, and the reduction of precious metal precipitate by reagents and other pyrometallurgical methods have been utilized in this case.

7.1.2 Recovery of Precious Metals

Various methods have been employed for the recovery of precious metals. Methods which have been applied to the recovery of gold and other precious metals from their solution are shown in Table 7.1.

Table 7.1: Recovery methods of gold.

Methods Name	Reference
Zinc dust cementation	Wan and Miller, 1990, Miller et al., 1990
Carbon adsorption	Xu et al., 1995
Electrodeposition	Wan and Miller, 1986
Solvent extraction	Mooiman and Miller, 1991
Ion exchange	Gomes et al., 2001

Table 7.2: Recovery methods of other precious metals.

Metal	Method	Reference
Silver	Precipitation	
	ion exchange	(Amberl and Murr, 1966
	reductive exchange	and Cotton and Ikinson, 1972
	electrolytic recovery	
Platinum group metals (PGM)	solvent extraction	Barnes and Edwards, 1982
	ion exchange	Els et al., 2000, Iglesias et al., 1999 and Rovira and Hurtado, 1998
	membrane separation	Takahiko et al., 1996
	Adsorption	Liu et al., 2000 and Veglio and Beolchini, 1997.

In recent years, attention has been focused on research related to bioadsorption, which is a cost effective biological method that has been demonstrated to possess good potential to replace conventional methods for recovery of precious metals using various biosorbents.

7.2 Gold Bioadsorption and Bioadsorbents of Gold

7.2.1 Gold Bioadsorption

The mechanisms of bioadsorption are generally based on physico-chemical interactions between metal ions and the functional groups present on the cell surface, such as electrostatic interactions, ions exchange and metal ion chelation and complexation (Ozer et al., 2004). The status of biomass, types of biomaterials, properties of metal solution chemistry, ambient/environmental conditions etc. influence the mechanism of metal bioadsorption. Bioadsorption of gold from solutions can be categorized as physical adsorption mechanism and chemical adsorption mechanism or chemisorption.

The binding mechanism of gold with tannin gel particles was highlighted by Ogata and Nakano (2005). The results suggested that a redox reaction between tannin gel and AuCl^{4-} was responsible for reduction of Au (III) ions to Au (0) ions and oxidation of hydroxyl groups of the tannin gel to carbonyl groups.

Bioadsorption properties of chemically modified chitosan were studied by Donia et al. (2007). Uptake of 3.6 mmol/g gold was reported through a series of experiments conducted in batch and column mode. Since the uptake process took place in a strong acid medium, the dominant mechanism of interaction was probably due to salt formation ($\text{R}-\text{CH} = \text{NH}^+ \text{AuCl}^{4-}$). Persimmon peel gel is also a gold recovering agent as studied by Parajuli et al. (2007).

The X-ray spectroscopic studies indicated that binding might be occurred through a nitrogen or oxygen ligand. Arrascue et al. (2003) studied that in acidic solutions, chitosan was protonated and protonated amine groups were available for sorption of anionic gold species. Glutaraldehyde

cross-linked chitosan could enhance the mechanism but the sorption capacity strongly decreased with increasing pH.

Spectroscopic studies were carried out by Romero-González et al. (2003) using dealginate seaweed waste on bioadsorption of gold (III). Colloidal gold was formed on the surface of dealginate seaweed by reduction of Au (III) to Au (0). Four different types of gold particles such as hexagonal platelets, tetrahedral, rods and decahedral were clearly identified by ESEM spectroscopy. The presence of nearly 75% of colloidal gold was measured through X-ray absorption fine structure (EXAFS) spectroscopy. Reduction of gold from Au (III) to Au (I) and Au (0) was also confirmed by the measured bond distances characteristic of the metal.

XRD and FTIR spectroscopic analysis was used by Atia et al. (2005) to study the bioadsorption mechanism of Au^{3+} ions on waste biomass of *Saccharomyces cerevisiae*. FTIR spectrophotometry demonstrated that active groups, such as the hydroxyl group of saccharides and the carboxylate anion of amino-acid residues from the peptidoglycan layer on the cell wall were the sites for the Au(III) binding, and the free aldehyde group acted as the electron donor for reduction of Au(III) to Au(0).

7.2.2 Bioadsorbents of Gold

Some researchers have investigated the recovery of gold using biosorbents as listed in Table 7.3.

Table 7.3: Bioadsorbents of gold.

Bioadsorbents	Reference
Algae	Hosea et al., 1986 ; Kuyucak and Volesky, 1989
Fungi	Gomes et al., 1998 ; Matsumoto and Nishimura, 1992
Yeasts	Karamuchka and Gadd, 1999

Activated carbon has also been used to adsorb gold from aqueous solution. However, its manufacturing and regenerating poses several constraints and represents a major portion of the operating cost in a mining operation (Kuyucak et al., 1986).

7.2.2.1 Algae

Algae have been proved to be efficient and economical biosorbent for the recovery of gold from aqueous solution. Au (III) was successfully recovered as metallic gold nanoparticle using dead biomass of the brown alga, *Fucus vesiculosus* (Mata et al., 2009). *Chlorella vulgaris*, a green algae was capable of removing more than 90% of the gold from very dilute solution (Hosea et al., (1986) and Ting et al., (1995)). The brown marine alga *Sargassum natans* was also found to be highly selective for gold (Kuyucak and Volesky, 1990).

7.2.2.2 Fungi

The fungal cells of *Aspergillus niger*, *Mucor rouxii* and *Rhizopus arrhizus* were found to take up precious metals like gold ((Mullen et al., 1992) and (Townsley and Ross, 1986)). Two strains of a fungus, *Cladosporium cladosporoides* 1 and *C. cladosporoides* 2 showed preferential sorption of gold (Pethkar et al., 2001). The fruiting body of a bracket fungi (*Fomitopsis carneae*) immobilized in polyvinyl alcohol was used as biosorbent and the gold (III) recovery was found to be 94 mg/g (Khoo and Ting, 2001). Out of 17 different fungal strains, *A. oryzae*, *Chaetomium globosum*, *Giberella fujikuroi*, *Mucor hiemalis*, *Penicillium chrysogenum* and *P. lilacinum* showed good bioadsorption capacity of gold (Tsuruta, 2004).

7.2.2.3 Yeasts

Among the 19 actinomycetes strains, *Streptomyces phaeochromogenes* HUT6013 showed maximum bioadsorption of gold (282 $\mu\text{mol/g}$ dry wt cells). Gold bioadsorption capacities of 14 strains of different yeast species viz. *Candida krusei*, *C. robusta*, *C. utilis*, *Cryptococcus albidus*, *C. laurentii* *Debaromyces hansenii*, *Endomyces fibigera*, *Hansenula anomala*, *H. saturnas*, *Kluyveromyces Pichia farinose*, *Saccharomyces cerevisiae*, *Sporobolomyces salmonicolor* and *Torulopsis aeria* were also reported (Tsuruta, 2004). Au^{3+} bioadsorption by waste biomass of *Saccharomyces cerevisiae* have been reported by Lin et al. (2005). The yeast biomass showed remarkable affinity for the gold ions due to its oxygenous functional groups on the cell wall.

7.2.2.4 Plant Biomass

The plant biomass like alfalfa biomass which was able to reduce gold (III) to Gold (0) was reported by Gardea-Torresdey et al. (2002). Gold (III) recovery from multi-elemental solutions was also reported by Gamez et al. (2003). Chemically modified hop biomass was evaluated for binding and reduction of Au (III) by López et al. (2005). The use of persimmon peel gel for the recovery of Au (III) from aqueous chloride medium was investigated by Parajuli et al. (2007).

Table 7.4 summarizes the different types of adsorbents used for gold bioadsorption.

Table 7.4: Bioadsorption of gold using different adsorbents.

Adsorbents	pH	Q _{max} (mmol/g)	Reference
<i>Fucus vesiculosus</i>	7.0	0.35	Mata et al. (2009)
<i>Dealginate Seaweed Waste</i>	3.0	0.4	Romero-González et al. (2003)
<i>Sargassum fluitans</i>	2.0	0.0032	Niu and Volesky (1999)
<i>Chlorella vulgaris</i>	6-7	0.5	Cordery et al. (1994)
<i>Sargassum natans</i>	2.5	2.1	Kuyucak and Volesky (1988)
<i>Ascophyllum nodosum</i>	2.5	0.15	Kuyucak and Volesky (1988)
<i>Chlorella vulgaris</i>	2.0	0.5	Darnall et al. (1986)
<i>C. cladosporioides Strain 1</i>	4.0	0.4	Pethkar et al. (2001)
<i>Streptomyces erythraeus</i>	4.0	0.03	Savvaidis (1998)

<i>Spirulina platensis</i>	4.0	0.026	Savvaidis (1998)
Rice husk carbon	-	0.76	Chand et al. (2009)
Chemically modified chitosan	-	3.4	Donia et al. (2007)
Crosslinked chitosan resin chemically modified with l-lysine	-	70.34 mg/g	Fujiwara et al. (2007)
Bisthiourea derivative of resins	2.0	3.63	Atia (2005)
Condensed-tannin gel	2.0	40.0	Ogata and Nakano (2005)
Alfalfa	5.0	0.18	Gomez et al. (2003)
Sulphur derivative of chitosan (RADC)	3.2	3.2	Arrascue et al. (2003)
Glutaraldehyde crosslinked chitosan (GCC)	1.6	2.9	Arrascue et al. (2003)
Hen eggshell membrane (ESM)	3.0	0.67	Ishikawa et al. (2002)
Dealginate Seaweed Waste	3.0	0.4	Romero et al. (2003)

7.3 Cellulose Based Bioadsorbents from Paper and Cloth

7.3.1 Paper

Paper is produced by pressing together moist fibers, typically cellulose pulp derived from wood, rags or grasses, and drying them into flexible sheets. Paper is a versatile material with many uses. Whilst the most common is for writing and printing upon, it is also widely used as a packaging material, in many cleaning products, in a number of industrial and construction processes, and even as a food ingredient – particularly in Asian cultures. Paper, and the pulp papermaking process, was said to be developed in China during the early 2nd century AD by the Han court eunuch Cai Lun, although the earliest archaeological fragments of paper derive from the 2nd century BC in China.

Table 7.5 shows a general composition of cellulose and others that can be found in paper.

Table 7.5: The natural composition of native wood and the pulps (Roberts, 1988).

Pulping process	Tree species	Cellulose (%)		Hemicellulose (%)		Lignin (%)		Extractives (%)	
		Wood	Pulp	Wood	Pulp	Wood	Pulp	Wood	Pulp
Sulfite	Spruce	41	78.1	30	17.1	27	3.8	2	1.0
	Birch	40	81.6	37	12.2	20	4.1	3	2.1
Kraft	Pine	39	73.3	30	18.9	27	6.3	4	1.1
	Birch	40	63.6	37	31.8	20	3.7	3	0.9

7.3.2 Cloth

The chemical composition of cotton fiber consists of 95% cellulose, 1.3% protein, 1.2% ash, 0.6% wax, 0.3% sugar, and 0.8 percent organic acids, and other chemical compounds that make up 3.1%. The non-cellulose chemicals of cotton are usually located in the cuticle of the fiber.

The non-cellulose chemicals of cotton consist of protein, ash, wax, sugar and organic acids. Cotton wax is found on the outer surface of the fiber. The more wax found on cotton the greater the surface area of cotton there is; finer cotton generally has more cotton wax. Cotton wax is primarily long chains of fatty acids and alcohols. The cotton wax serves as a protective barrier for the cotton fiber. Sugar makes up 0.3% of the cotton fiber, the sugar comes from two sources plant sugar and sugar from insects. The plant sugars occur from the growth process of the cotton plant. The plant sugars consist of monosaccharide, glucose and fructose. Organic acids are found in the cotton fiber as metabolic residues. They are made up of malic acid and citric acid.

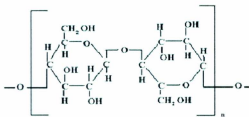


Figure 7.1: Chemical structure of cotton.

CHAPTER 8

8 Materials and Methods

8.1 Materials

Analytical grade chloride salts of copper, iron, zinc, nickel, lead and palladium were used to prepare test solutions of respective metals. Analytical grade of HAuCl₄.4H₂O and H₂PtCl₆.6H₂O were used to prepare gold and platinum solutions, respectively. All other chemicals used for the preparation of adsorbent and for adsorption tests were of analytical grade and were used without further purification.

8.2 Preparation of Adsorption Gel from Cloth and Paper

Daily used cloth and shredded paper were used in the present study as the raw material to prepare cellulose gel. For the preparation of the gel, 10 g of each thing was suspended in 50 ml of concentrated sulfuric acid (18M) in a round bottom flask and the mixture was stirred for 24 h at 373 K for cross-linking condensation reaction. After that, the mixture was cooled at room temperature and was neutralized with 5M NaOH, followed by washing several times with distilled water until neutral pH. The black product obtained was dried in a convection oven for 24 h at 343 K. Then, the gel was passed through the 150 µm mesh size of testing sieve for regulating the uniform particles.

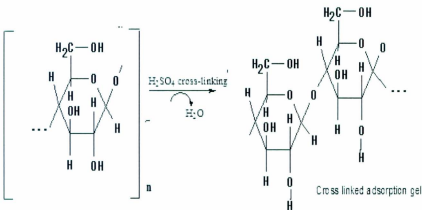


Figure 8.1: Synthetic route of cross-linked adsorption gel.

8.3 Measurement and Analysis

The pH and concentration of metal solution were measured by using ORION 5STAR series pH meter, calibrated with buffers of pH 1.0, 2.0, 4.0 and 7.0 on a regular basis and a Perkin Elmer optima Inductive Couple Plasma Optical Emission Spectrometer (ICPOES), respectively. Reproducibility of all adsorption experiments was confirmed by repeating the same adsorption test.

The characterization of the adsorbents before and after adsorption was done by Rigaku Ultima IV X-ray diffractometer with a copper X-ray source and a scintillation counter detector, Bruker TENSOR 27 infrared spectrometer and FEI Quanta 400 environmental Scanning Electron Microscope.

8.4 Batch Adsorption Test

In the present investigation, batch mode of operation was conducted in order to measure the adsorption behaviors of gold and other metal ions individually. Thus, in a representative experiment, 10 mg of dried gel was shaken together with 10 ml of each metal ion solution (0.2 mM) at varying hydrochloric acid concentration at 303 K for 24 h. After equilibrium, the mixture was filtered and the filtrate was analyzed for remaining metal ion concentration.

Percentage adsorption for each metal ion was calculated according to Eq. (8.1), where C_i and C_e (mM) represents the initial and equilibrium concentration, respectively. The amount of adsorbed Au (III) (Q , mmol/g) was calculated by the mass balance calculation of Au (III) before and after the adsorption as expressed by Eq. (8.2).

$$\% A = \frac{C_i - C_e}{C_i} \times 100 \quad \dots \dots \dots \quad (8.1)$$

$$Q = \frac{C_i - C_e}{M} \times V \quad \dots \dots \dots \quad (8.2)$$

Where V (ml) is the volume of the test solution used and W (g) is the dry weight of the adsorbent.

8.5 Kinetic Studies

For the measurement of kinetics of adsorption, 200 mg of gel was mixed together with 200 mL of solution containing 0.2 mM of Au (III) in 1 M hydrochloric acid and stirred by using a magnetic stirrer at 298 K. Each 15 mL solution was sampled at definite time intervals from the start of the operation. Similar experiments were also carried out at 298, 303, 313 and 323 K.

In order to evaluate the activation energy of the present adsorption reaction, the pseudo-first order rate constant evaluated at different temperatures were plotted according to the Arrhenius equation as shown in Eq. (8.3).

$$\ln k = \ln A - \frac{E_a}{RT} \quad \dots \dots \dots \quad (8.3)$$

Where, A represents the frequency factor, R is the universal gas constant, E_a is the activation energy (kJ mol^{-1}) and T is the absolute temperature (K).

8.6 Isotherm and Kinetic Models

Adsorption isotherms of Au(III) were measured by shaking 10 mg (dry weight) of the gel in 10 mL solutions of 1 M hydrochloric acid varying the initial concentration of Au(III) in the range of 0.5-6 mM at four different temperatures (298, 303, 313 and 323 K) for 96 h.

Langmuir model is presented by Eq. (8.4).

$$q_e = \frac{q_m b C_e}{(1+bC_e)} \dots \quad (8.4)$$

Where, q_e and q_m are the equilibrium and maximum metal adsorption of metal ion per unit weight of adsorbent to form a complete monolayer on the surface bound at C_e ; respectively; b is the equilibrium constant.

From the evaluated values of b at varying temperature, some thermodynamic parameters, changes in the free energy (ΔG°), enthalpy (ΔH°) and entropy (ΔS°) associated to the adsorption process were evaluated according to the Eqs. (8.5) and (8.6).

$$\Delta G^\circ \equiv -RT \ln b \quad (8.5)$$

$$\ln b = \Delta G^\circ / RT \equiv -\Delta H^\circ / RT + \Delta S^\circ / R \quad \dots \quad (8.6)$$

The plot $\ln b$ as a function of I/T as shown yields a straight line with the correlation coefficient (r^2), from which the values of ΔH° and ΔS° can be calculated from the slope and intercept, respectively. The more negative of ΔG° , the stronger the driving force of the adsorption reaction. The decrease in the value of ΔG° with the increase of temperature shows that the reaction is more spontaneous at a high temperature, which indicates that the adsorption processes are favored by the increase in temperature. Positive value of enthalpy (ΔH°) demonstrates the endothermic nature of the adsorption. Entropy, as the measure of randomness of the system, also indicates the positive values suggesting the increased mechanism of gold (III) adsorption.

For speed up the reaction time by increasing solid liquid ratio, 200, 1000 and 1600 mg of gel was mixed together with each 200 mL of solution containing 1 mM of Au (III) in 1 M hydrochloric acid and stirred by using a magnetic stirrer at 323 K. Each 15 mL solution was sampled at definite time.

8.7 XRD Analysis

XRD analysis was performed on Rigaku Ultima IV X-ray diffractometer with a copper X-ray source. The Ultima IV, with Rigaku's patented Cross Beam Optics (CBO), is a flexible, multi-purpose XRD. It incorporates fully automatic alignment and allows for fast, easy switching between focusing and parallel beam geometries without the need to reconfigure the system. Other features of the Ultima IV at Memorial University are the automatic 10-position sample changer with spinner and the high temperature (1500 °C) attachment. The experiments were carried out at The Earth Resources Research and Analysis (TERRA) Facility, Memorial University of Newfoundland.

8.8 FT-IR Analysis

FT-IR analysis was performed on Bruker TENSOR 27 infrared spectrometer. This instrument has a spectral range of 7,500 to 370 wave numbers and is equipped with a Miracle ATR accessory allowing rapid and easy analysis of liquid and solid samples. The experiments were carried out at The Centre of Chemical Analysis, Research and Training (C-CART) at Memorial University of Newfoundland.

8.9 Scanning Electron Microscope (SEM) Analysis

Scanning Electron Microscope Analysis was performed on FEI Quanta 400 environmental SEM. The term environmental refers to this SEM's capability for working at near atmospheric pressures instead of high vacuum. This capability allows for almost any specimen to be examined, including wet and non-conducting specimens.

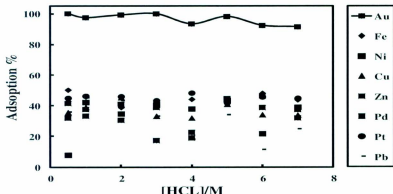
For accommodating the variety of information available from electron interaction, SEM is also equipped with an energy dispersive X-ray (EDX) analytical system from Roentec, an electron backscatter diffraction (EBSD) system from HKL, and mineral liberation analysis (MLA) software from JKTech at the University of Queensland Australia. The experiments were carried out at Micro Analysis Facility-INCO Innovation Centre (MAF-IIC), Memorial University of Newfoundland.

CHAPTER 9

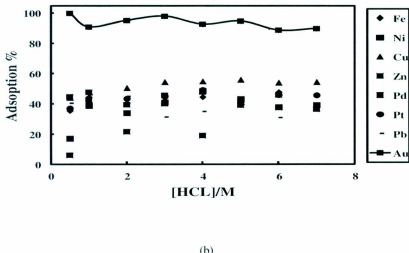
9 Results and Discussions

9.1 Influence of [HCl] for the Metal Adsorption

It is obvious from Figure 9.1(a) and (b) that almost 100% adsorption of Au(III) was achieved in the low concentration range of hydrochloric acid while the extents of adsorption of other precious and base metals studied were very insignificant over the whole hydrochloric acid concentration regions. Thus, it is evident that both of the adsorption gel has a high affinity and selectivity for Au(III). From the viewpoint of selectivity and extent of Au(III) adsorption, the obtained result is quite interesting and it is expected to selectively recovery Au(III) separated from a number of other precious and base metals as tested in the present work.



(a)

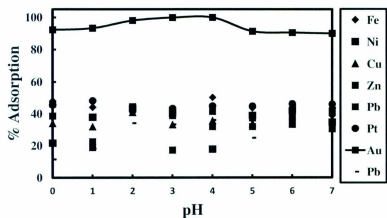


(b)

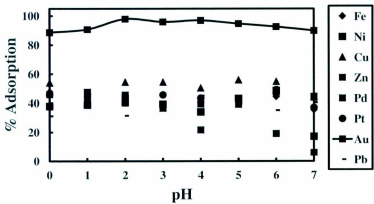
Figure 9.1: Adsorption of metals ions on (a) cloth gel, (b) paper gel as a function of hydrochloric acid concentration. *Conditions:* weight of dry gel = 10 mg, volume of HCl solution = 10 mL, concentration of metals = 0.2 mM, shaking time = 24 h, temp = 303 K.

9.2 Effect of pH on Metal Adsorption

Figure 9.2 shows the effect of equilibrium pH on the adsorption of various metal ions by (a) cloth gel and (b) paper gel at an initial metal concentration of 0.2 mM. The result shows that optimum adsorption for metals have taken place in the pH region of 1 to 4. The pH decreased after adsorption in all cases, this suggests that uptake of metal ions takes place according to an ion exchange mechanism.



(a)

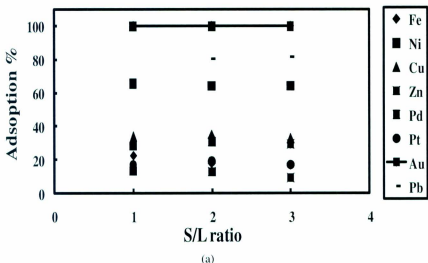


(b)

Figure 9.2: Adsorption of metals ions on (a) cloth gel, (b) paper gel as a function of pH.
 Conditions: weight of dry gel = 10 mg, volume of HCl solution = 10 mL, concentration of metals = 0.2 mM, shaking time = 24 h, temp = 303 K

9.3 Effect of Solid/Liquid Ratio on Metal Adsorption

Figure 9.3 shows the effect of solid liquid ratio on the adsorptive removal of the metal ions by the (a) cloth gel, and (b) paper gel at the initial pH of 1. Adsorption does not change with the increases of solid liquid ratio.



(a)

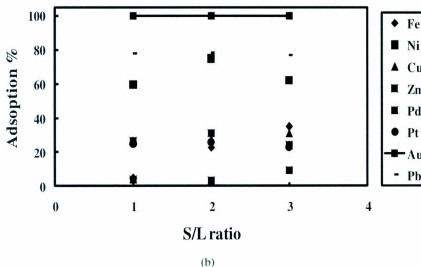
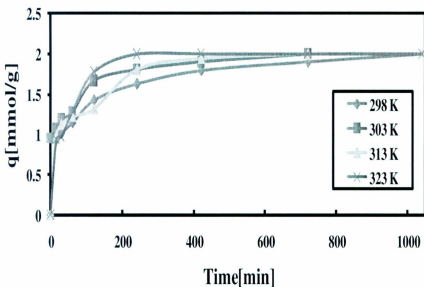


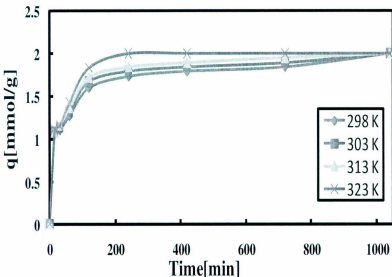
Figure 9.3: Removal of metal ions from aqueous solution on the a) cloth gel, b) paper as a function of solid/liquid ratio. Weight of the gel= 20, 40, 60 mg. Initial pH= 3.5. Volume of the aqueous solution= 20 mL.

9.4 Adsorption Isotherms

As it was found that the gel is selective only for Au(III) ions, further experimental works were carried out only for Au(III) ions. The data of adsorption kinetics of Au(III) is illustrated in 9.4(a) for cloth gel and (b) for paper gel shows the variation of the amount of Au(III) adsorbed on the gel as the function of shaking time at different temperature. It is observed from these figs. that temperature has a significant effect on the adsorption rate of Au(III). The time required to reach adsorption equilibrium is shortened with increasing temperature. Furthermore, it is seen that the adsorption rapidly increases at the initial stages and then the adsorption rate is slowed down to zero at the final stages for all the temperatures tested. Since the equilibrium reached nearly within 240 min for all temperatures studied for the present gel, the contact time was fixed at 24 h in the following experiments in order to completely ensure the adsorption equilibrium.



(a)

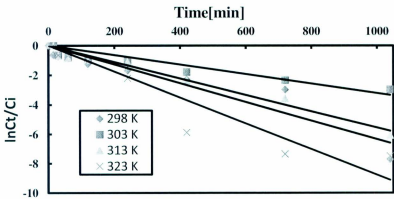


(b)

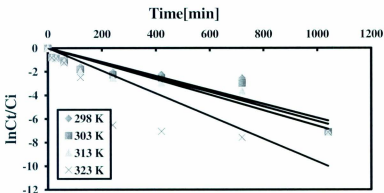
Figure 9.4: Adsorption rate of Au (III) by the cloth adsorption gel at different temperatures.

Conditions: Weight of the dry gel = 200 mg, volume of the solution = 200 mL, concentration of Au (III) = 0.2 mM, HCl concentration = 1 M (a) on cloth gel and (b) on paper gel.

The kinetic data at the initial stage were re plotted on the basis of the pseudo-first order kinetic model according to Eq. (8.3) as shown in Fig. 9.5 (a) for cloth and (b) for paper. In this figure, nearly all plots appear to cluster on the straight lines passing through the origin corresponding to different temperatures. From the slopes of these straight lines, the pseudo-first order rate constants were evaluated at four different temperatures.

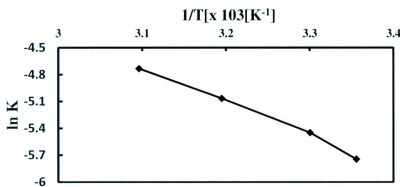


(a)

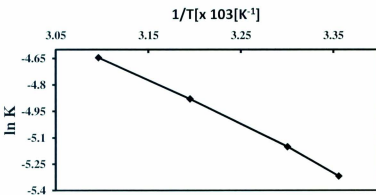


(b)

Figure 9.5: Adsorption rate of Au (III) by the adsorption gel at different temperatures. Pseudo-first order plot. *Conditions:* Weight of the dry gel = 200 mg, volume of the solution = 200 mL, concentration of Au (III) = 0.2 mM, HCl concentration = 1 M (a) on cloth gel, and (b) on paper gel.

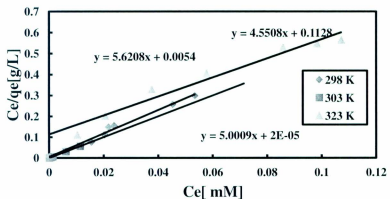


(a)

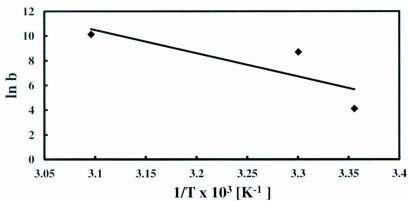


(b)

Figure 9.6: Adsorption rate of Au (III) by the adsorption gel at different temperatures. Arrhenius plot. *Conditions:* Weight of the dry gel = 200 mg, volume of the solution = 200 mL, concentration of Au (III) = 0.2 mM, HCl concentration = 1 M (a) on cloth gel, and (b) on paper gel.

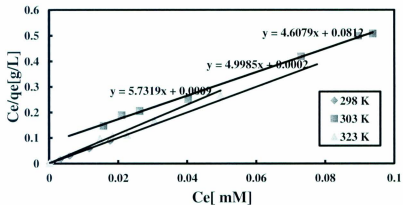


(a)

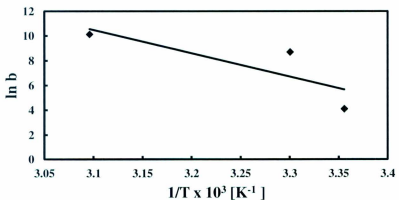


(b)

Figure 9.7: Adsorption isotherms at different temperature (a) Langmuir Plots and (b) Van's Hoff plot for cloth gel.



(a)



(b)

Figure 9.8 Adsorption isotherms at different temperature (a) Langmuir Plots and (b) Van's Hoff plot for paper gel.

Table 9.1: Thermodynamic parameters for the adsorption of Au (III) on cloth adsorbent gel.

T (K)	b L/mmol	lnb	q mmol/g	ΔG KJmol ⁻¹	ΔH KJmol ⁻¹	ΔS JK ⁻¹ mol ⁻¹	R ²
298	44.34775	3.792062	1.9999	-18.1478	-177.637	637.185	0.8278
313	1970.701	7.586145	1.999				
323	26359.91	10.1796	1.9999				

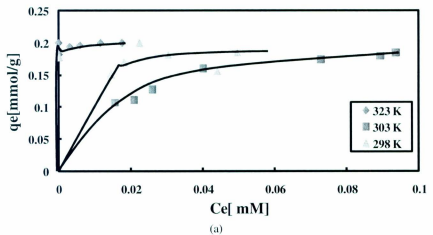
(a)

Table 9.2: Thermodynamic parameters for the adsorption of Au (III) on paper adsorbent gel.

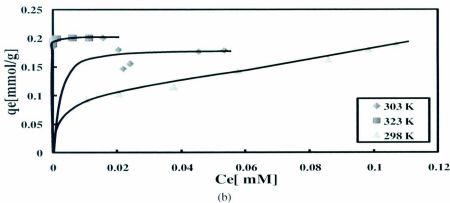
T (K)	b L/mmol	lnb	q mmol/g	ΔG KJmol ⁻¹	ΔH KJmol ⁻¹	ΔS JK-1mol ⁻¹	R ²
298	61.68585	4.122055	1.9999				
313	6028.491	8.704252	1.999	-19.3625	-155.813	570.1242	0.6675
323	25023.9	10.12759	1.9999				

Figure 9.9 (a, b) presents the adsorption isotherms of Au (III) ions at various Temperature.

The adsorption capacity increased with increasing equilibrium concentration of metal.



(a)

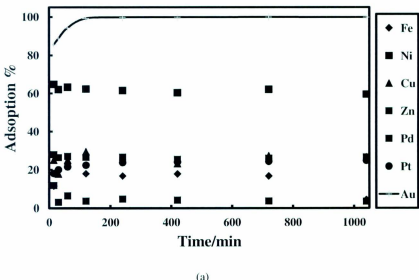


(b)

Figure 9.9: Adsorption isotherms of Au (III) onto cotton gel at different temperatures. (a) For cloth and b) for paper. *Conditions:* weight of dry gel = 10 mg, volume of solution = 10 mL, shaking time = 24 h, HCl = 0.1 M.

9.5 Kinetic Studies

Figure 9.10 illustrates the evolution of metal uptake with time for two different gels. Adsorption occurs mainly within the first 240 min. Faster kinetics has significant practical importance as it will facilitate the scale up of the process to small reactor volumes, ensuring efficiency and economy. This behavior is typical of biosorption of gold involving purely weak intermolecular forces between the biomass and the metal in solution.



(a)

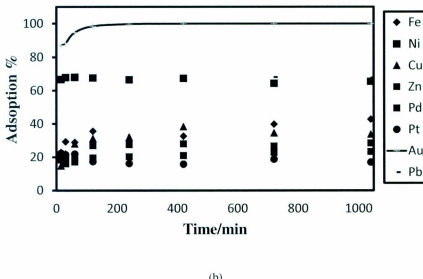
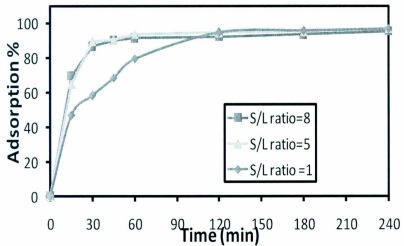


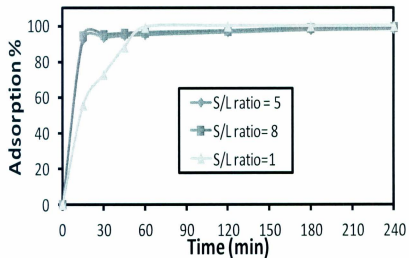
Figure 9.10: Adsorption kinetics of different metal a) on cloth gel, and (b) on paper gel.

9.6 Effect of Increasing Solid Liquid Ratio to Increase the Reaction Time

Figure 9.11 shows the reaction kinetics at different solid/liquid ratio for cloth and paper gel, respectively. In both cases when the solid/liquid ratio is higher or equal to five the reaction time decreased considerably. Like for S/L ratio 1 it takes almost 120 min to finish 90% of the adsorption but for solid liquid ratio 5 and 8 it happened only at first fifteen minutes, which is acceptable at industrial range.



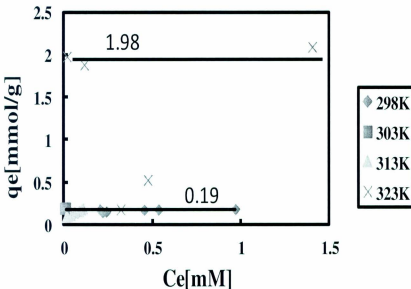
(a)



(b)

Figure 9.11: Adsorption kinetics at different sample of different solid liquid ratio.(a) on cloth gel and (b) on paper gel.

A higher adsorption capacity of 1.98 mol kg^{-1} and 1 mol kg^{-1} was also found for cloth and paper respectively using higher solid liquid ratio .



(a)

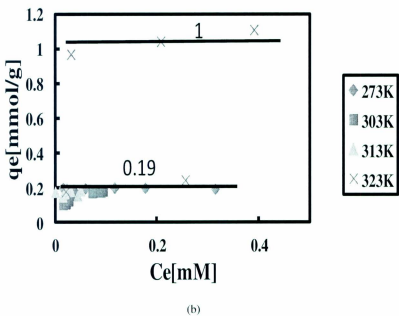


Figure 9.12: Adsorption isotherms at different sample of higher solid liquid ratio.(a) on cloth gel, and (b) on paper gel.

9.6 Proposed Mechanism of Metal Adsorption

It is evident from the results that Au(III) were strongly adsorbed on cloth and paper gel at pH 1-3 whereas it was poorly adsorbed at alkaline pH, suggesting the possibility of elution of metal using alkaline solution, from which it is suggested that the adsorption mechanism of metal on cellulose gel is interpreted shown in Fig. 9.13.

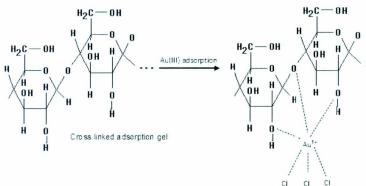


Figure 9.13 : Adsorption mechanism of Au(III) ions on cellulose based gel.

9.8 XRD Analysis

XRD is a bulk method and reveals information on the bulk structure of the metal and its adsorbent. The following profiles were processed: (111), (200), (220) and (311). Their experimental relative intensities with respect to the 2θ values are shown in Figs. 9.14 and 9.15 for cloth and paper respectively. These results explain the metal features of the bulk gold investigated clusters despite the strong deformation of the crystalline structure. By XRD method one can obtain the crystallite size that has different values for different crystallographic planes.

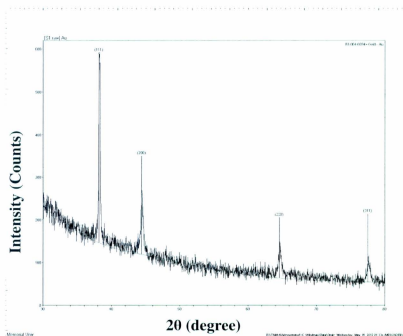


Figure 9.14: XRD pattern of a cloth adsorbent gel containing Au(III).

The Au pattern displayed the reflexions characteristic of f.c.c. crystal structure. Starting from thermal treatment at 300 °C, the patterns displayed the reflexions characteristic of gold f.c.c. crystal structure.

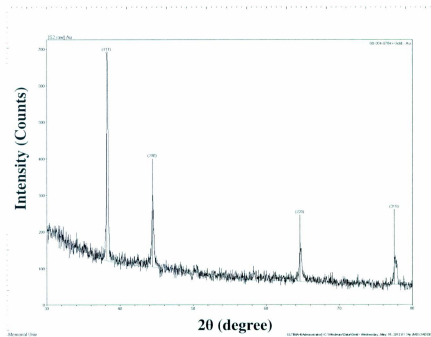


Figure 9.15: XRD pattern of a paper adsorbent gel containing Au(III).

9.9 FT-IR Analysis

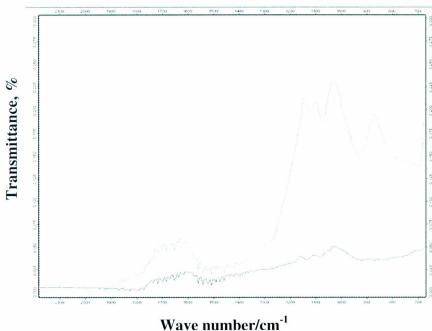


Figure 9.16: FT-IR Spectrum of cloth adsorbent gel before and after gold adsorption.

IR analysis permits spectrophotometric observation of the adsorbent structure in the range of 400-4000 cm^{-1} and serves as a direct means for the identification of functional groups on the surface. An examination of the adsorbent before and after adsorption reaction possibly provides information regarding the surface groups that might have participated in the adsorption reaction and also indicates the surface sites on which adsorption have taken place. FT-IR spectra of the cloth and paper gel before and after Au(III) adsorption were taken (Figure 9.16 and 9.17) in order to understand the structural change as well as the involvement of main functional group.

Both spectra show the peak at around 1000-1200 cm⁻¹ which clearly indicate the presence of Au in the gel.

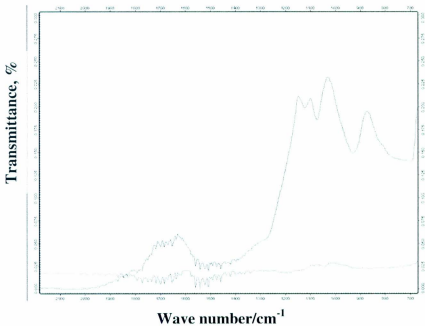


Figure 9.17: FT-IR Spectrum of paper adsorbent gel before and after gold adsorption.

9.10 SEM Analysis

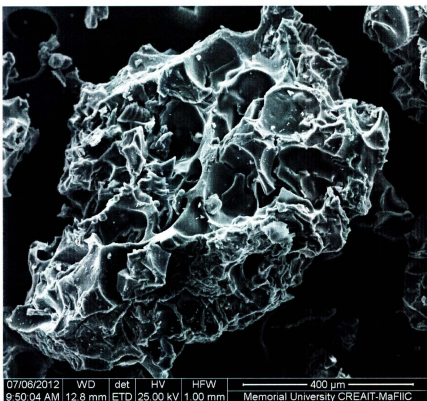
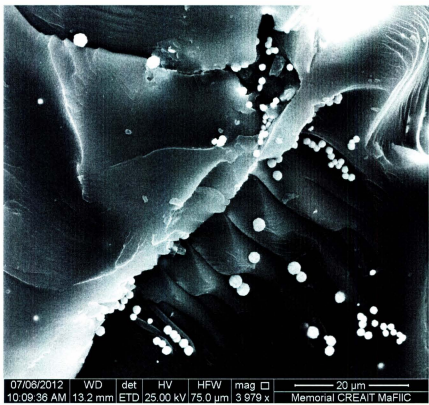


Figure 9.18: SEM photograph of cloth adsorbent gel before gold adsorption.



07/06/2012 WD det HV HFW mag □ — 20 μ m —
10:09:36 AM 13.2 mm ETD 25.00 kV 75.0 μ m 3.979 x Memorial CREAT MaFiC

Figure 9.19: SEM photograph of cloth adsorbent gel after gold adsorption. Magnification:4000X



07/06/2012	WD	det	HV	HFW	mag	□	10 μm
10:31:51 AM	13.2 mm	ETD	25.00 kV	30.0 μm	9 947 x		Memorial CREAT MaFiC

Figure 9.20:SEM photograph of cloth adsorbent gel after gold adsorption, Magnification:10000X

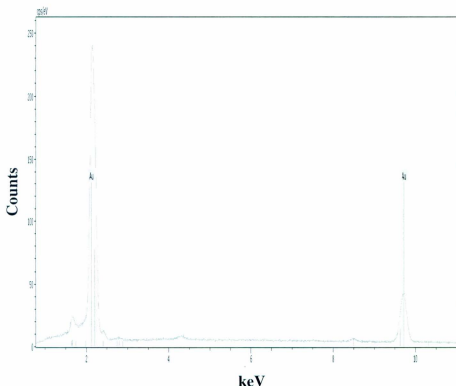
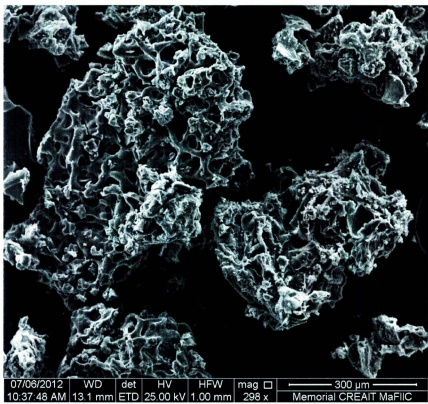
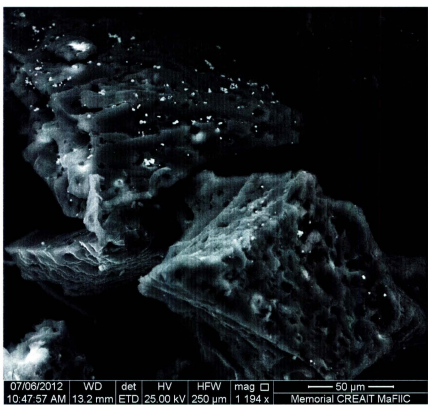


Figure 9.21: EDX analysis of cloth adsorbent gel with gold by SEM.



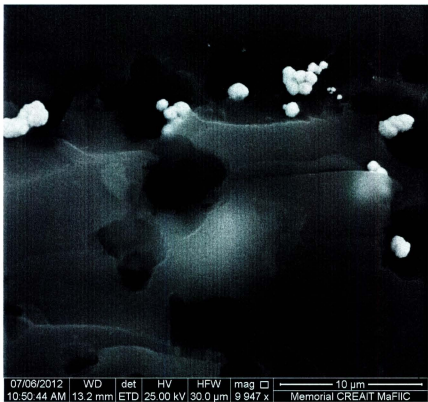
07/06/2012 WD det HV HFW mag □ 300 μm
10:37:48 AM, 13.1 mm ETD 25.00 kV 1.00 mm 298 x Memorial CREAT MaFIC

Figure 9.22: SEM photograph of paper adsorbent gel before gold adsorption.



07/06/2012	WD	det	HV	HFW	mag	□	50 µm
10:47:57 AM	13.2 mm	ETD	25.00 kV	250 µm	1 194 x		Memorial CREAT MaEIC

Figure 9.23: SEM photograph of paper adsorbent gel after gold adsorption. Magnification: 1100X



07/06/2012 | WD | det | HV | HFW | mag | 10 μ m
10:50:44 AM | 13.2 mm | ETD | 25.00 kV | 30.0 μ m | 9,947 x | Memorial CREAT MaFiC

Figure9.24:SEM photograph of paper adsorbent gel after gold adsorption. Magnification:10000X

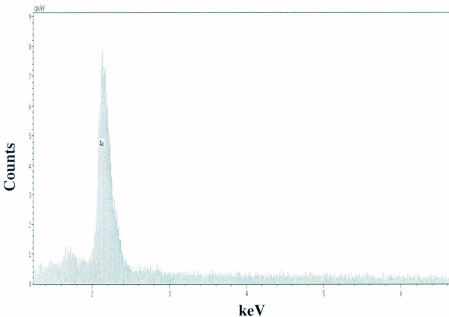


Figure 9.25: EDX analysis of paper adsorbent gel with gold by SEM.

The SEM images of the cloth and paper before and after Au adsorption are presented in Figs. 9.18 and 9.22 , respectively that reveal randomly distributed pore structures for cloth and paper gel. Evidence of large internal surface areas in the microporous structures within the gels is presented in those figures. The SEM image in Figs. 9.19, 9.20, 9.23 and 9.24 are present cloth and paper gel after metal adsorption and the presence of numerous inner micropores. From the image it can be seen that there is a highly microporous structures in gel which can provide the maximum number of possible Au loading sites.

The EDX analysis graphs at Figs. 9.21 and 9.25 clearly show the presence of Au in cloth and paper only after adsorption.

9.11 Research Findings

In this work, we investigate the cellulose base bioadsorbent using cloth and paper as an extractant to uptake gold from any waste solution. As a waste we used the synthetic solution of different pH, concentration and temperature. Cloth and paper are a cellulose rich bio-polymer than can be chemically modified by Sulphuric acid which can act like an anion exchanger when it is loaded with Au ions. The results of the adsorption experiments suggest that those jels can be applied for uptaking gold from wastewater as an rescuer of valuable metals.

From the above results, we have shown that both cloth and paper jel was effective in uptaking the Au from solution, indicating the complete uptake of Au. Our result can be applied in waste management areas, by which a huge amount of valuable and rare metal can uptake. The concept of these adsorbents is not unique, but using it as an adsorbent to uptake gold from waste solution is a new thing. Cloth and paper cellulose was chosen as biosorbent due to its special structure, insolubility in water, chemical stability and local availability. The core findings of this research are:

- Gold was almost completely uptaken from synthetic solution by chemically modified cloth and paper gel.
- The effective pH range was found to be 1 to 4.
- Platinum and Paladium are also uptaken from the waste solution to a significant amount.

- The maximum loading capacities for Au (III) were found to be 1.98 and 1 molkg⁻¹ by cloth and paper respectively.
- The gold uptake depends on the pH, sorbent dosage and initial concentrations.
- The adsorption capacity increased with increasing equilibrium concentration of metal.

CHAPTER 10

10 Conclusion and Recommendation

10.1 Conclusion

Biosorption of precious metals from solutions has received great deal of attention in the recent years. When compared with the conventional methods, a biosorption-based process offers a number of advantages including low operating costs, minimization of the volume of chemical and/or biological sludge to be handled and high efficiency in detoxifying effluents. Selective separation and recovery of Au (III) away from any other precious or base metal ions can be achieved by using crosslinked cloth and paper gel. The excellent selectivity and high capacity of this gel provides a cost effective and environment friendly method for gold recovery. The adsorption isotherm clearly indicated that the reaction product has an adsorptive capacity and was capable of recovering 388 g/kg gold of reaction product. This adsorption follows a Type I process and fits the assumptions of the Langmuir isotherm. Kinetics data on the adsorbent determined that the Au(III) uptake was very rapid, with maximum uptake occurring at approximately the 240-min mark. These tests also demonstrated the dependence of the adsorption process on the initial concentration of Au(III) in solution, with uptake rising with increased concentration. Further examination revealed a correlation of the process to the pseudo-second-order kinetics model. It was notable, however, that the overall rate constants and the initial adsorption rates decreased as a result of higher initial concentrations of Au(III). The

adsorption process was shown not to be affected significantly by temperature and the ideal pH of adsorption was shown to be pH 1-4. Increasing in solid liquid ratio more than five times resulted 90% of the adsorption that happened within the first 15 min which shows its acceptability in industrial scale. Also, the enhanced capacity of cellulose based gel and its selectivity for Pd (II) and Pt (IV) is an adventitious point for the recovery of traces of valuable metals. These findings suggest that cellulose based gel exhibits significant potential as an adsorbent for the recovery of precious metals from industrial waste.

10.2 Proposals for the Future Work

In this research, all experiments were conducted batch wise. But for effectiveness to recover gold from industrial Waste, it will be necessary to do the tests by continuous column method. And for industrial application a sustainable process flow with low adsorption time and final gold recovery with adsorbent recycling should be done for maximum utilisation of this environment friendly bioadsorbent.

REFERENCE

Acid Mine Drainage, 2012: Retrieved 3 June, 2012, from Wikipedia Web site:

http://en.wikipedia.org/wiki/Acid_mine_drainage

Copper_toxicity, 2012: Retrieved 3 June, 2012, from Wikipedia Web site:

http://en.wikipedia.org/wiki/Copper_toxicity

Fourier_transform_infrared_spectroscopy, 2012: Retrieved 3 June, 2012, from Wikipedia Web site: http://en.wikipedia.org/wiki/Fourier_transform_infrared_spectroscopy

Lead_poisoning, 2012: Retrieved 3 June, 2012, from Wikipedia Web site:

http://en.wikipedia.org/wiki/Lead_poisoning

Mining, 2012: Retrieved 3 June, 2012, from Wikipedia Web site:

<http://en.wikipedia.org/wiki/Mining>

Precious_metal, 2012: Retrieved 3 June, 2012, from Wikipedia Web site:

http://en.wikipedia.org/wiki/Precious_metal

Scanning_electron_microscope, 2012: Retrieved 3 June, 2012, from Wikipedia Web site:

http://en.wikipedia.org/wiki/Scanning_electron_microscope

XRD, 2012: Retrieved 3 June, 2012, from University of New Mexico Web site:

<http://epswww.unm.edu/xrd/xrdbasics.pdf>

Abidin, M.A.Z., Jalil, A.A., Triwahyono, S., Adam, S.H., Kararudin, N.H.N. (2011). Recovery of gold(III), from an aqueous solution onto a *Durio zibethinus* husk, *Biochemical Engineering Journal*, **54**, 124-131.

Alloway, B. J. (1990). Soil processes and the behaviour of metals. *Heavy Metals in Soils*. Blackie and Son Ltd., Glasgow, Britain. 7-28.

Alloway, B. J. (1992). Biochemistry of trace metals.

Alloway, B.J, Ayres, D.C. (1993). Chemical principles of Environmental Pollution. Blackie Academic U.K . 140-149.

Arden, E., Lockett, W.T. (1914). Experiments on the oxidation of sewage without the aid of filters, *J. Soc. Chem. Ind.* 33, 0523-539.

Arrascue, M.L., Garcia, H.M., Horna, O., Guibal, E. (2003). Gold sorption on chitosan derivatives. *Hydrometallurgy* 71, 191–200.

Atia, A., Donia, A.M., Yousif, A.M. (2005). Comparative study on the recovery of silver (I). from aqueous solutions using different chelating resins derived from glycidyl methacrylate. *Journal of Applied Polymer Science* 97 (3),, 806–816.

Barnes, J.E., Edwards, J.D. (1982). Solvent extraction at Inco's Action precious metal refinery. *Chemistry and Industry* 6, 151.

Batty, A.J., Dixon, K.W., Brundrett, M.C., Sivasithamparam, K. (2002). Orchid conservation and mycorrhizal associations. *Microorganisms in Plant Conservation and Biodiversity*. 195-226.

- Bayramoglu, G., Denizli, A. , Bektas, S., Arica M.Y. (2002). Entrapment of *Lentinus sajor-caju* into Ca-alginate gel beads for removal of Cd(II) ions from aqueous solution: preparation and biosorption kinetics analysis. *Microchemical* 72 , 63–76.
- Berner, R.A. (1980). Early diagenesis. Princeton.
- Chand, R., Wateri, T., Inoue, K., Kawakita, H., Luitel, H.N., Parajuli, D., Torikai, T., Yada, M. (2009). Selective adsorption of precious metals from hydrochloric acid solutions using porous carbon prepared from barley straw and rice husk. *Minerals Engineering* 22, 1277–1282.
- Cheung, C.W., Porter, J.F., McKay, G. (2001). Sorption kinetic analysis for the removal of cadmium ions from effluents using bone char. *Water Research* 35, 605–612
- Chockalingam , Subramanian, S. (2006). Studies on removal of metal ions and sulphate reduction using rice husk and *Desulfovomaculum nigricans* with reference to remediation of acid mine drainage, *Chemosphere*, 62, 699–708.
- Clarke, L.B. (1995). Coal Mining and Water Quality. London7 IEA. *Coal Research*, 99
- Cordery, J., Will, A.J., Atkinson, K., Wills, B.A. (1994). Extraction and recovery of silver from low grade liquirs using microalgae. *Minerals Engineering* 7 (8),, 1003–1015.
- Corti, C.W. , Holliday, R.J. (2004). Commercial aspects of gold applications: from materials science to chemical science. *Gold Bull* 37, 20–26.
- Cotton, E.A. , Ikinson, G.W. (1972). Advanced Inorganic Chemistry. 3rd edition. Wiley, New York, 721–725.

- Darnall, D.W., Greene, B., Henzl, M.T. (1986). Selective recovery of gold and other metal ions from an algal biomass. *Environmental Science and Technology* 20 (2), 206–208.
- Davis, T.A., Volesky, B., Mucci, A. (2003). A review of the biochemistry of heavy metal biosorption by brown algae. *Water Research* 37, 4311–4330.
- Dearing, S.(2009). Defunct for 20 years, Buchans NF mine source of toxic pollution. Digitaljournal.com.
- Dhakal, R.P., Ghimire, K.N., Inoue, K., Yano, M., Makino, K. (2005). Acidic polysaccharide gels for selective adsorption of lead(II) ion. *Sep. Purif. Technol.*, 42,219– 225.
- Dhakal, R.P.,Ghimire, K.N., Inoue, K. (2005). Adsorptive seperation of heavy metals from an aquatic environment using orange waste.*Journal of Hydrometallurgy*, 79, 182-190.
- Dobson, R.S. , Burgess, J.E. (2007). Biological treatment of precious metal refinery wastewater: a review. *Minerals Engineering* 20, 519–532.
- Donia, A.M., Atia, A.A., Elwakeel, K.Z. (2007). Recovery of gold (III), and silver (I), on a chemically modified chitosan with magnetic properties. *Hydrometallurgy* 87, 197–206.
- Drever, J.I. (1988). The geochemistry of natural waters (second edition).: Englewood Cliffs, New Jersey, Prentice-Hall. 437 .
- Dunbabin, J.S., Bowmer, K.H. (1992). Potential use of constructed wetlands for treatment of industrial wastewaters containing metals. *The Science of the Total Environment* 111, 151–68.
- Els, E.R., Lorenzen, L., Aldrich, C. (2000). The adsorption of precious metals and base metals on a quaternary ammonium group ion exchange resin. *Minerals Engineering* 13, 401.

- Esposito, A., Pagnanelli, F., Lodi, A., Solisio, C., Veglio, F. (2001). Biosorption of heavy metals by *Sphaerotilus natans*, an equilibrium study at different pH and biomass concentrations, *Hydrometallurgy* 60, 129–141.
- Fiset, J.F., Zinek, J.M., Nkinamubanzi, P.C. (2003). Chemical stabilization of metal hydroxide sludge. *Proceedings of the X International Conference on Tailings and Mine Waste*, October 2003, Vail, CO, USA, AA Balkema. 329-332.
- Fujiwara, K., Ramesh, A., Maki, T., Hasegawa, H., Ueda, K. (2007). Adsorption of platinum (IV), palladium (II), and gold (III), from aqueous solutions on L-lysine modified crosslinked chitosan resin. *Journal of Hazardous Materials* 146, 39–50.
- Fyson, A., Kalin, M., Adrian, L.W. (1994). Arsenic and nickel removal by wetland sediments. *Proc. 3rd International Conf on Abatement of Acidic Drainage*, April 24-29, 1994, Pittsburgh, PA, USA, USBM SP 06A-94, 109-118.
- Gadd, G.M., White, C., DeRome, L. (1988). Heavy metal and radionuclide uptake by fungi and yeasts. R. Norri, D.P. Kelly (Eds.), *Biohydrometallurgy*, Chippenham, Wilts, UK.
- Gamez, G., Gardea-Torresdey, J.L., Tiemann, K.J., Parsons, J., Dokken, K. (2003). Recovery of gold (III), from multi-elemental solutions by alfalfa biomass. *Advances in Environmental Research* 7 (2), 563–571.
- Gardea-Torresdey, J.L., Tiemann, K.J., Parsons, J.G., Gameza, G.I., Herrera, M., Jose-Yacaman, M. (2002). XAS investigations into the mechanism(s) of Au (III) binding and reduction by alfalfa biomass. *Microchemical Journal* 71, 193–204.

- Gomes, N.C.M., Camargos, E.R.S., Dias, J.C.T., Linardi, V.R. (1998). Gold and silver accumulation by *Aspergillus niger* from cyanide containing solution obtained from the gold mining industry. *World Journal of Microbiology and Biotechnology* 14, 149.
- Gomes, C.P., Almeida, M.F., Loureiro, J.M. (2001). Gold recovery with ion exchange used resins. *Separation and Purification Technology* 24 (1–2), 35–57.
- Grohmann, K., Baldwin, E. A. (1992). "Hydrolysis of orange peel with pectinase and cellulase enzymes," *Biotechnol. Lett.* 14, 1169-1174.
- Groudev, S. N., Bratcova, S. G., Komnitsas, K. (1999). Treatment of waters polluted with radioactive elements and heavy metals by means of a laboratory passive system. *Minerals Engineering* 12(3): 261-270.
- Ho, Y.S., McKay, G. (1999). Pseudo second order model for sorption process. *Process Biochemistry* 34 , 451–465.
- Hosea, M., Greene, B., McPherson, R., Henzel, M., Alexander, M.D., Darnall, D.W. (1986). Accumulation of elemental gold on the alga *Chlorella vulgaris*. *Inorganica Chimica Acta* 123, 161–165.
- Hussein, A., Mahvi, Naghipour, D., Vaezi, F., Nazmara, S. (2005). Tea waste as an adsorbent for heavy metal removal from industrial wastewaters. *Am. J. Appl. Sci.*, 2 (1), 372– 375.
- Iglesias, M., Antic'ó, E., Salvad'ó, V. (1999). Recovery of palladium (II) and gold (III) from diluted liquors using the resin duolite GT-73. *Analytica Chimica Acta* 381, 61.
- Ishikawa, S.I., Suyama, K., Arihara, K., Itoh, M., (2002). Uptake and recovery of gold ions from electroplating wastes using eggshell membrane. *Bioresource Technology* 81, 201–206.

- Jacobsen, R.T. (2005). Removing contaminants from spent catalysts. *Chemical Engineering Progress* 101, 20–23.
- Jamode, A.V., Rao, M., Chandak, B.S., Jamode, V.S., Parwate, A.V. (2003). Applications of the inexpensive adsorbents for the removal of heavymetals from industrial waste water: a brief review. *J. Ind. Pollut. Control* 19 (1), 114–134.
- Kadlec, R.H., Keoleian, G.A. (1986). Metal ion exchange on peat. *Peat Water*, 61–93.
- Kamel, S., Hassan, E.M., El-Sakhawy, M. (2006). Preparation and application of acrylonitrile-grafted cyanoethyl cellulose for the removal of copper(II) ions. *Journal of Applied Polymer Science* 100, 329–334.
- Kalin, R.M. (2004). Engineered passive bioreactive barriers: risk-managing the legacy of industrial soil and groundwater pollution. *Current Opinion in Microbiology* Vol 7, No. 3, 227–238
- Karamuchka, V. , Gadd, G.M. (1999). Interaction of *Saccharomyces cerevisiae* with gold toxicity and accumulation. *BioMetals* 12, 289–294.
- Khoo, K.H., Ting, Y.P. (2001). Biosorption of gold by immobilized fungal biomass. *Biotechnology and Bioengineering Journal* 8, 51–59.
- Kiyoyama, S., Maruyama, T., Kamiya, N., Goto, M. (2008). Immobilization of proteins into microcapsules and their adsorption properties with respect to precious metal ions, *Ind. Eng. Chem. Res.* 47, 1527-1532.
- Kleinmann, R.L.P., Hedin, R.S. (1993). Treating mine water using passive method. *Journal of Pollution Engineering* 25 (13), 20–22.

- Klemm, D., Schmauder, H.P., Heinze, T., Cellulose , Baets, S. D., Vandamme, E.J., Steinbuchel, A. (2002). Polysaccharides II. Polysaccharides from Eukaryotes, vol. 6Wiley-VCH, Weinheim, 275–320.
- Kuyucak, N., Volesky, B. (1986). Rao, U.V. (Ed.), Proceedings of the 10th International Precious Metals Institute Conference. Lake Tahoe, NV. 211–216.
- Kuyucak, N., Volesky, B. (1988). Biosorbents for recovery of metals from industrial solutions. *Biotechnology Letters* 10 (2), 137–142.
- Kuyucak, N., Volesky, B., 1989. Accumulation of gold by algal biosorbent. *Biorecovery* 1, 189–204.
- Kuyucak, N., Volesky, B. (1990). Biosorption of algal biomass. In: Volesky, B. (Ed.)., Biosorption of heavy metals. CRC Press, Boca raton.
- Lambert, J., Murr, T.A. (1966). Practical Chemistry, 2nd Edition. Heinemann, London 67, 336–364.
- Larous,S., Meniai, A.H., Lehocine, M.B. (2005). Experimental study of the removal of copper from aqueous solutions by adsorption using sawdust. *Desalination* 185, 483–490.
- López, M.L., Parsons, J.G., Videau, J.R., Gardea-Torresdey, J.L. (2005). An XAS study of the binding and reduction of Au(III) by hop biomass. *Microchemical Journal* 81, 50–56.
- Leyva-Ramos,R., Bernal-Jacome, L.A., Acosta-Rodriguez, I.(2005). Adsorption of cadmium (II). from aqueous solution on natural and oxidized corncob. *Separation and Purification Technology* 45 , 41–49.

- Lin, Z., Wu, J., Xue, R., Yang, Y. (2005a). Spectroscopic characterization of Au³⁺ biosorption by waste biomass of *Saccharomyces cerevisiae*. *Spectrochimica Acta* 61, 761–765.
- Lin, Z., Zhou, C., Wu, J., Zhou, J., Wang, L. (2005b). A further insight into the mechanism of Ag⁺ biosorption by *Lactobacillus* sp. strain A 09. *Spectrochimica Acta* A61, 1195–1200.
- Liu, Y.Y., Fu, J.K., Zhou, Z.H. (2000). A study of Pt4+ adsorption and its reduction by *Bacillus megaterium*. *Chemical Research in Chinese Universities* 16 (3), 246.
- Luo, F., Liu, Y.H., Li, X.M., Xuan, Z.X., Ma, J.T. (2006). Biosorption of lead ion by chemically-modified biomass of marine brown algae *Laminaria japonica*. *Chemosphere* 64, 1122–1127.
- Machemer, S.D., Wildeman, T.R. (1992). Adsorption compared with sulfide precipitation as metal removal processes from acid mine drainage in a constructed wetland. *Journal of Contaminant Hydrology*, 9: 115-131.
- Mao, J., Won, S.W., Vijayaraghavan, K., Yun, Y.S., (2009). Surface modification of *Corynebacterium glutamicum* for enhanced Reactive Red 4 biosorption. *Bioresource Technology* 100, 1463–1466.
- Mata, Y.N., Torres, E., Blázquez, M.L., Ballester, A., González, F., Muñoz, J.A. (2009). Gold (III) biosorption and bioreduction with the brown alga *Fucus vesiculosus*. *Journal of Hazardous Materials* 166, 612–618.
- Matagi, S.V., Swai, D., Mugabe, R. (1998). A review of heavy metal removal mechanisms in wetlands. *Afr. J. Trop. Hydrobiol. Fish* 8, 23–35.
- Matsumoto, M., Nishimura, Y. (1992). Recovery by *Aspergillus oryzae* of gold from wastewater gold plating. *Nippon Nōugeikagakukaishi* 66, 1765–1770 in Japanese.

- McDowall, D.J., Gupta, B.S., Stannett, V.T. (1984). Grafting of vinyl monomers to cellulose by ceric ion initiation. *Progress in Polymer Science* 10 (1), 1–50.
- Miller, J.D., Wan, R.Y., Parga, J.R. (1990). Characterization and electrochemical analysis of gold cementation from alkaline cyanide solution by suspended zinc particles. *Hydrometallurgy* ...24, 373–392.
- Mooiman, M.B., Miller, J.D. (1991). The chemistry of gold solvent extraction from alkaline cyanide solution by solvating extractants. *Hydrometallurgy* 27, 29–46.
- Mullen, M.D., Wolf, D.C., Beveridge, T.J., Bailey, G.W. (1992). Sorption of heavy metals by the soil fungi Aspergillus niger and Mucor rouxii. *Soil Biology and Biochemistry* 24, 129–135.
- Müller, G. (1988). Chemical decontamination of dredged materials, combustion residues, soil and other materials contaminated with heavy metals. In: Wolf, W. J., Van de Brink, Colon, F. J. ed. 2nd international TNO/BMFT conference on contaminated soil Vol. 2. Kluwer Dordrecht, Amsterdam, Holland. 1439-1442.
- Murphy, V., Hughes, H., McLoughlin, P. (2008). Comparative study of chromium biosorption by red, green and brown seaweed biomass. *Chemosphere* 70, 1128–1134.
- Neal, C., Whitehead, P.G., Jeffery, H., Neal, M. (1994). The water quality of the River Carnon, west Cornwall, November 1992 to March 1994: the impacts of Wheal Jane discharges. *Sci Total Environ.*
- Niu, H., Volesky, B. (1999). Characteristics of gold biosorption from cyanide solution. *Journal of Chemical technology and Biotechnology* 74, 778–784.

- Ogata, T., Nakano, Y. (2005). Mechanisms of gold recovery from aqueous solutions using A novel tannin gel adsorbent synthesized from natural condensed tannin. *Water Research* 39, 4281–4286.
- Ozer, A., Ozer, D., Ekiz, H.I. (2004). The equilibrium and kinetic modeling of the biosorption of copper (II) ions on *Cladophora crispata*. *Adsorption* 10, 317–326.
- Parajuli, D., Kawakita, H., Inoue, K., Ohto, K., Kajiyama, K. (2007). Persimmon peel gel for the selective recovery of gold. *Hydrometallurgy* 87, 133–139.
- Patrick Jr., W. H. and M. Verloo, (1998). Distribution of soluble heavy metals between ionic and complexed forms in saturated sediment as affected by pH and redox conditions. *Water Science and Technology* 37 (6/7).: 165-172.
- Pethkar, A.V., Paknikar, K.M. (1998). Recovery of gold from solutions using *Cladosporium cladosporioides* biomass beads. *Journal of Biotechnology* 63, 121–136.
- Pethkar, A.V., Kulkarni, S.K., Paknikar, K.M. (2001). Comparative studies on metal biosorption by two strains of *Cladosporium cladosporioides*. *Bioresource Technology* 80, 211–215.
- Ramesh, A., Hasegawa, H., Sugimoto, W., Maki, T., Ueda, K. (2008). Adsorption of gold (III), platinum(IV), and palladium(II), onto glycine modified crosslinked chitosan resin. *Bioresource Technology* 99, 3801–3809.
- Regine, H.S.F.V. , Boya, V. (2000). Biosorption: a solution to pollution? *Journal of Int. Microbiol*, 3: 17–24.
- Roberts, J.C. (1988). The Chemistry of Paper. 2nd Edition.

- Romero-González, M.E., Williams, C.J., Gardiner, P.H.E. (2003). Spectroscopic studies of the biosorption of gold(III), by dealginate seaweed waste. *Environmental Science and Technology* 37 (18), 4163–4169.
- Rovira, M., Hurtado, L. (1998). Recovery of palladium from hydrochloric acid solutions using impregnated resins containing alamine 336. *Reactive and Functional Polymers* 38, 279.
- Saeed, M., Iqbal, M., Akhtar, M.W. (2005). Removal and recovery of lead (II), from single and multimetals (Cd, Cu, Ni, Zn), solutions by crop milling waste (black gram husk)., *Journal of Hazardous Materials* B117, 65–73.
- Savinov, V.M., Gabrielsen, G.W., Savinova, T.N. (2003). Cadmium, zinc, copper, arsenic, selenium and mercury in seabirds from the Barents Sea: levels, inter-specific and geographical differences. *Science of the Total Environment* 306, 133–158.
- Savvaidis, (1998). Recovery of gold from thiourea solutions using microorganisms. *BioMetals* 11, 145–151.
- Takahiko, K., Masahiro, G., Fumiuki, N. (1996). Separation of platinum and palladium by liquid surfactant membranes utilizing a novel bi-functional surfactant. *Journal of Membrane Science* 120, 77.
- Tam, N.F.Y., Wong, Y.S. (1994). Mangrove Ecosystems of Hong Kong and Pearl River Delta.
- Tangaromsuk, J., Pokethitiyook, P., Kruatrachue, M., Upatham, E.S. (2002). Cadmium biosorption by *Sphingomonas paucimobilis* biomass. *Bioresource Technology* 85, 103–105.
- Tewari, N., Vasudevan, P., Guha, B.K. (2005). Study on biosorption of Cr (VI), by *Mucor hiemalis*. *Biochemical Engineering Journal* 23, 185–192.

- Tipping, E., Hetherington, N. B., Hilton, J., Thompson, D. W., Bowles, E., Hamilton-Taylor, J. (1985). Artifacts in the use of selective chemical extraction to determine distributions of metals between oxides of manganese and iron. *Anal. Chem.* **57**, 1944-1946
- Thomas, A., Debusk, R. B., Laughlin, J., Schwartz, L. N. (1996). Retention and compartmentalization of lead and cadmium in wetland microcosms. *Water Research* **30**(11), 2707-2716.
- Ting, Y.P., Teo, W.K., Soh, C.Y. (1995). Gold uptake by Chlorella vulgaris. *Journal of Applied Phycology* **7**, 97-100.
- Townsley, C.C., Ross, I.S. (1986). Copper uptake in Aspergillus niger during batch growth and in non-growing mycelial suspension. *Experimental Mycology* **10**, 281-288.
- Tsuruta, T. (2004). Biosorption and recycling of gold using various microorganisms. *Journal of General and Applied Microbiology* **50**, 221-228
- Veglio, F., Beolchini, F. (1997). Removal of metals by biosorption: a review. *Hydrometallurgy* **44**, 301.
- Volesky, B. (1990). Biosorption of heavy metals. CRC Press, Boca Raton, FL, USA.
- Volesky, B. (2001). Detoxification of metal-bearing effluents: Biosorption for the next century. *Hydrometallurgy* **59**, 203-216.
- Wakelyn, P. (2006). Cotton Fiber Chemistry and Technology. CRC Press, 15-18.
- Wan, R.Y., Miller, J.D. (1986). Solvation extraction and electrodeposition of gold from cyanide solutions. *Journal of Metals*, 35-40.

- Wan, R.Y., Miller, J.D. (1990). Research and development activities for the recovery of gold from alkaline cyanide solutions. *Mineral Processing and Extractive Metallurgy Review* 6, 143–190.
- Wiebner, A., U. Kappelmeyer, P., Kuschk, M., Kastner, (2005). Influence of the redox condition dynamics on the removal efficiency of a laboratory-scale constructed wetland. *Water Research* 29, 248–256.
- Woulds, C., Ngwenya, B.T. (2004). Geochemical processes governing the performance of a constructed wetland treating acid mine drainage, Central Scotland. *Applied Geochemistry* 19 (11), 1773–1783.
- Xu, Q., Meng, X., Han, K.N. (1995). The electrochemical behavior of the dissolution of gold–silver alloys in cyanide solutions. SME, Denver, CO, USA.
- Yano, M., Inoue, K. (1997). Adsorption of metal on alginic acidamide, pectic acid amide, cross linked pectic acid and crosslinked alginic acid. *Anal. Sci.* 13, 359–360.
- Yano, M., Inoue, K., Makino, K., Baba, Y. (2001). Kankyokagakukaishi (Japanese). 14, 345–349.
- Younger, P.L., Jayaweera, A., Elliot, A., Wood, R., Amos, P., Daugherty, A.J. (2003). Passive treatment of acidic mine waters in subsurface flow systems: exploring RAPS and permeable reactive barriers. *Land Contam Reclam* 11, 127–135.
- Zhou, D., Zhang, L.N., Guo, S.L. (2005). Mechanisms of lead biosorption on cellulose/chitin beads. *Water Research* 39, 3755–3762.

APPENDIX A

**Experimental Result for Removals of Heavy Metals from Acid Mine
Drainage (AMD) using Bioadsorbent from Orange Waste**

Table A1: ICP results on water samples of different metal concentrations

file =	0						
run =	waters						
owner =	A.Bertin(w2377)/M.Hossain(w2376)						
date =	Nov 30 10 16:09 pm						
calculated:	01-Dec-10 11:34:22						
waters (w), biol. (b):	w						
avg dln g/g:	0.032011						
conc given in:	ppb						
conc in:	wet						
interference correction?							
intf. factor							
ppm intf.							
lld - intf.							
lld - ppb/ppm							
lld - blank							
bk average							
Sample name	Li	7	Be	B	Mg	Al	Si
	ppm	ppm	ppm	ppm	ppm	ppm	ppm
bnano-1		0.012	<0.00	<0.00	0	0.02	<0.3
t145		0.03	0.011	0.045	8.43	0.06	4.9
t155		0.036	<0.00	0.103	11.72	0.07	4.7
t191		0.004	0.005	0.042	3.71	0.06	1.9
b nano-3		<0.00	<0.03	<0.02	0.00	<0.0	<2
m34774h	A1	0.052	<1.96	<1.64	1.00	<1.6	<150
m34775b	A2	0.207	<2.00	<1.68	1.00	<1.6	<154
m34776v	A3	0.227	<1.90	<1.60	1.00	<1.5	<146
m34777p	A4	<0.13	<1.86	<1.56	1.00	<1.5	<142
m34778j	A5	<0.13	<1.89	<1.59	1.00	<1.5	<145
m34779d	R1	<0.13	<1.95	<1.64	<0.2	<1.6	<149
m34780h	R2	0.406	<1.88	<1.58	1.00	<1.5	<144
m34781e	R3	<0.13	<1.91	<1.61	2.0	4.02	5
m34782a	R4	0.146	-0.193	<1.62	0.0	<1.6	<148
m34783x	R5	0.152	<1.96	<1.65	1.0	<1.6	39
m34783x dup		0.159	<1.92	<1.62	<0.2	<1.6	33
m34784u	S1	<0.13	<1.94	<1.63	12.0	8.84	<149
m34785q	S4	<0.14	<2.05	<1.72	15.0	6.14	<157
m34786n	S5	0.167	<1.95	<1.64	11.0	4.07	<150
m34787j	B1	<0.13	<1.93	<1.62	11.0	4.77	68
m34788g	B2	<0.14	<1.97	<1.65	15.0	4.14	<151
m34789c	B3	0.18	<1.93	<1.62	10.0	2.03	-5

Table A1: ICP results on water samples of different metal concentrations(contd.)

Cl									
P	S	Cl	Ca 43	Ti	V	Cr 52	Fe 54	Mn	
ppm	ppm	ppm	ppm	ppm	ppm	ppm	ppm	ppm	ppm
<0.0	<5	<1	<0	<0.00	<0.00	0.001	<0.13	<0.00	
<0.0	8.47	41	29	<0.00	0.01	0.015	0.2	0.021	
<0.0	20.27	24	46	<0.00	0.025	0.01	<0.13	0.056	
<0.0	18.95	14	29	<0.00	0.001	0.004	<0.13	0.027	
<0	-6	<3	<1	<0.03	<0.00	<0.00	<1	<0.00	
<12	-1817	<264	<77	<2.15	<0.21	<0.17	<66	0.1	
<12	<2646	<270	99	<2.20	<0.22	<0.17	<67	<0.05	
<12	<2514	<257	<75	<2.09	<0.20	<0.16	<64	<0.05	
<11	<2451	<250	<73	<2.04	<0.20	<0.16	<62	<0.05	
<12	<2501	<256	123	<2.08	<0.20	0.182	<64	0.1	
<12	<2572	<263	<76	<2.14	<0.21	<0.17	<65	0.1	
<12	<2484	<254	<74	<2.06	<0.20	<0.16	<63	0.1	
<12	<2527	<258	<75	1.021	<0.21	<0.16	<64	0.092	
<12	<2543	<260	<75	0.304	<0.21	<0.16	<65	<0.05	
<12	<2590	278	<77	<2.15	<0.21	<0.17	<66	<0.05	
<12	<2539	<259	<75	<2.11	<0.21	<0.16	<65	<0.05	
<12	<2562	-61	<76	<2.13	<0.21	<0.16	<65	2.001	
<13	<2705	<276	<80	<2.25	<0.22	<0.17	<69	1.818	
<12	<2575	<263	78	<2.14	<0.21	0.192	<66	1.372	
<12	<2547	<260	<76	<2.12	<0.21	<0.16	<65	1.784	
<12	<2598	<266	<77	<2	<0.21	<0.17	<66	1.715	
<12	<2543	-229	85	<2	<0.21	<0.16	<65	1.172	

Table A1: ICP results on water samples of different metal concentrations (contd.)

Ca	Ca	Ca				
97700	52983	8127				
4	4	4				
0.403	2.492	2.658				
0.0621	0.2574	0.4217				
0.148	1.435	0.926	4.439	0.117		

Co	Ni	Cu	Zn	Pb	Sample	
ppm	ppm	ppm	ppm	ppm	diln g/g	
0.001	<0.00	<0.00	0.005	0	0.107651	
0	0.015	0.007	0.011	0.013	0.10844	
0	0.009	0.037	0.066	0.02	0.106489	
0	0.002	<0.00	0.049	0.002	0.104297	
0.002	<0.00	0.004	0.014	<0.00	0.015927	
2	0.298	2.585	11.123	0.113	0.000205	
0	<0.24	8.212	18.321	0.364	0.0002	
<0.02	<0.22	27.80	35.941	0.765	0.00021	
0	<0.21	50.36	67.508	1.193	0.000216	
0	<0.22	64.892	88.662	1.617	0.000211	
0	<0.23	7.796	97.504	4.406	0.000206	
<0.02	<0.21	15.32	23.052	4.522	0.000213	
0.05	<0.22	48.416	44.358	40.572	0.000209	
0.03	<0.22	78.04	73.599	5.752	0.000208	
0.033	<0.23	92.58	10.912	53.503	0.000204	
<0.02	<0.23	90.69	8.634	54.416	0.000208	
0.028	<0.23	0.931	28.794	1.287	0.000206	
<0.03	<0.24	2.813	36.731	2.884	0.000196	
0.032	<0.23	1.223	27.828	0.264	0.000205	
0.026	<0.23	0.202	15.336	0.049	0.000208	
0.032	0.553	0.711	30.924	0.136	0.000204	
0.075	-0.136	0.323	17.837	0.028	0.000208	

Table A2: ICP results on water samples of different solid liquid ratio

Water sample 2 Date: 27/01/2011

Name	Copper	Lead	zinc
C11	0.9	0.03	2.31
C12	2.88	0.14	5.14
C13	4.16	0.31	3.85
C31	11.78	0.12	28.49
C32	31.86	1.74	45.45
C33	39.87	3.47	42.2
C51	47.39	1.9	77.97
C52	86.32	0.57	89.46
C53	90.47	8.16	90.72

Table A3: ICP results on water samples of different pH

Sample ID	Description	Cu 324.752	%RSD	Pb 220.353	%RSD	Zn 206.200	%RSD
ES001453	43	35.26	1.92	5.12	2.33	50.76	1.76
ES001454	45	27.76	2.25	5.08	3.21	51.14	2.03
ES001455	46	37.73	2.26	47.06	0.66	42.21	2.45
ES001456	42	35.85	4.02	4.27	5.45	67.47	3.86
ES001457	41	84.58	2.08	3.81	1.34	74.79	2.04
ES001458	44	31.18	2.45	8.73	2.13	59.66	2.57
ES001459	47	22.12	0.04	7.49	3.45	61.27	0.46
ES001455d	46 duplicate	37.55	2.25	47.12	2.68	41.97	2.46
71A	multi element chk	10.02	1.06	10.45	1.54	10.05	1.17
accepted 71A		9.99		10.01		10.03	
given error 71A		0.03		0.04		0.05	

Table A4: ICP results on water samples of different time

Water sample: 4		Date: 18/03/2011		
Name		Copper	Zink	Lead
S11		2.209	20.013	1.735
S12		0.471	17.102	0.87
S13		0.329	23.876	0.974
S14		3.503	21.312	1.948
S15		0.542	13.495	0.425
S16		1.905	20.596	0.306
S21		0.84	22.888	0.765
S22		0.83	18.62	0.698
S23		0.008	17.387	0.421
S24		1.278	24.581	1.605
S25		0.84	15.202	0.548

APPENDIX B

**Experimental Results for Recovery of gold from synthetic solution using
cellulose base bioadsorbent from paper and cloth**

Table B1: ICP results on samples of different HCL concentrations

Name		Ca	Ti	V	Cr	Fe
		ppm	ppm	ppm	ppm	ppm
Limit of Detection		0	0.00	0.000	0.000	0.00
BNANO-I		0	0.00	0.000	0.000	0.00
PT-PD 1PPM		0	0.03	0.160	0.011	0.00
AU-1PPM		0	0.07	0.279	0.021	0.00
M36842K	C1	2	0.06	0.072	0.044	49.72
M36843F	C2	1	0.33	0.815	0.163	14.05
M36844A	C3	3	0.38	0.932	0.290	61.18
M36845W	C4	1	0.44	1.631	0.480	7.79
M36846R	C5	0	0.45	1.696	0.697	5.81
M36847N	C6	0	0.40	1.483	0.286	16.43
M36848I	C7	1	0.42	1.517	0.318	11.92
M36849E	C8	0	0.41	1.610	0.602	6.27
M36850G	P1	86	0.11	0.120	0.072	64.47
M36851K	P2	94	0.59	1.126	0.230	15.54

M36852O	P3	81	0.66	1.374	0.429	79.54
M36853S	P4	113	0.65	1.319	0.446	5.71
M36854W	P5	91	0.66	1.368	0.642	5.37
M36855A	P6	76	0.68	1.339	0.279	18.50
M36856E	P7	93	0.69	1.365	0.312	12.19
M36857I	P8	70	0.67	1.444	0.590	4.01

Table B1: ICP results on samples of different HCL concentrations (contd.)

O.Mehfuz w2478 , Environmental/Exploration RUN = 166; Dec19111						
		calculated on		21-Dec	2011	
Name		Co	Ni	Cu	Zn	As
		ppm	ppm	ppm	ppm	ppm
Limit of Detection		0	0.00	0.00	0.0	0.000
BNANO-1		0.00	0.00	0.0	0.012	0.000
PT-PD 1PPM		0.00	0.00	0.0	0.000	0.049
AU-1PPM		0.00	0.00	0.0	-0.001	0.063
M36842K	C1	0.01	276.39	44.4	68.147	0.028
M36843F	C2	0.01	143.44	21.0	42.485	0.275
M36844A	C3	0.01	195.93	34.7	59.086	0.315
M36845W	C4	0.01	59.11	46.8	31.210	0.415
M36846R	C5	0.01	36.42	48.0	81.110	0.418
M36847N	C6	0.01	49.28	193.1	56.495	0.402
M36848I	C7	0.01	234.90	46.0	53.782	0.405

M36849E	C8	0.01	183.33	16.2	32.694	0.428
M36850G	P1	0.02	448.23	55.8	93.904	0.042
M36851K	P2	0.01	63.46	27.4	52.310	0.348
M36852O	P3	0.01	287.92	49.4	78.280	0.406
M36853S	P4	0.01	56.80	45.5	29.806	0.408
M36854W	P5	0.01	33.92	45.0	80.825	0.411
M36855A	P6	0.03	50.11	64.0	58.480	0.432
M36856E	P7	0.01	66.19	35.908	54.005	0.443
M36857I	P8	0.02	61.99	15.454	32.839	0.436

Table B 1: ICP results on samples of different HCL concentrations (contd.)

Name	Mo ppm	Pd ppm	Ag ppm	Pt ppm	Au ppm	Pb ppm
C1	0.007	18.528	0.092	45.091	0.019	23.955
C2	0.004	26.793	0.727	43.749	8.918	14.707
C3	0.009	39.547	0.194	34.038	4.288	16.374
C4	0.009	82.756	0.406	36.691	3.991	96.652
C5	0.003	47.473	0.200	21.744	10.516	81.795
C6	0.000	55.416	0.195	28.196	4.704	65.822
C7	0.006	319.323	0.231	24.342	3.042	88.476
C8	0.008	38.135	0.211	25.219	7.344	75.046
P1	0.006	15.360	0.027	42.894	0.038	19.386
P2	0.002	27.173	0.984	40.278	3.609	13.735
P3	0.007	40.499	0.266	32.485	9.778	14.820
P4	0.008	74.336	0.450	34.798	8.682	28.520
P5	0.006	42.118	0.219	20.724	2.886	24.788
P6	0.000	50.755	0.226	28.600	6.002	20.370
P7	0.007	82.387	0.293	24.050	4.437	28.794
P8	0.008	33.444	0.228	24.211	7.955	21.850

Table B2: ICP results on water samples of different pH

Sample ID	Client ID	Dilution	Au	Au	Au		Mean
			mg/L	mg/L	mg/L		mg/L
Calibration blank			0.009	0.008	0.014		0.01
71C		10x	9.87	9.90	9.87		9.88
Exp. Conc.							10.0
ES001663	S1	20x	18.67	18.53	18.52		18.6
ES001664	S2	10x	24.32	24.16	24.06		24.2
ES001665	S3	10x	25.57	25.70	25.56		25.6
ES001666	S4	10x	16.89	16.92	16.92		16.9
Std 5.00 mg/L			4.906	4.91	4.892		4.90
Exp. Conc.							5.00
ES001667	S5	10x	18.77	18.83	18.85		18.8
ES001668	S6	10x	34.03	33.94	33.96		34.0
ES001669	S7	10x	23.42	23.36	23.4		23.4

Table B2: ICP results on water samples of different pH (contd.)

Calibration standards: 0.100, 0.500 and 1.00 mg/L						
Calibration blank			0.001	0.005	0.005	0.004
71C	10x		0.979	0.986	0.979	0.98
Exp. Conc.						1.00
ES001670	10x	P1	0.063	0.079	0.081	0.07
ES001671	10x	C1	0.031	0.052	0.049	< 0.05
ES001672	5x	P2	0.033	0.046	0.040	< 0.05
ES001673	5x	C2	0.018	0.027	0.028	< 0.05
Std 0.50 mg/L			0.490	0.495	0.493	0.49
Exp. Conc.						0.50
ES001674	5x	P3	0.624	0.616	0.616	0.62
ES001675	5x	C3	0.119	0.121	0.116	0.12
ES001676	5x	P4	0.018	0.035	0.026	< 0.05
ES001677	5x	C4	0.111	0.102	0.099	0.10
ES001678	5x	P5	2.157	2.164	2.165	2.16
Std 1.00 mg/L			0.966	0.970	0.967	0.97

Exp. Conc.						1.00
ES001679	5x	C5	0.260	0.255	0.262	0.26
ES001680	5x	P6	8.444	8.494	8.486	8.47
ES001681	5x	C6	2.251	2.232	2.239	2.24
ES001682	5x	P7	6.187	6.188	6.202	6.19
ES001683	5x	C7	1.198	1.219	1.23	1.22
ES001684	5x	P1	0.022	0.031	0.030	< 0.05
ES001685	5x	C1	0.010	0.019	0.014	< 0.05
ES001675	undiluted	C3	0.109	0.114	0.113	0.11

Table B3: ICP results on water samples of different time

Name		Ca	Ti	Cr	Fe	Mn
M36858M	C11	1	0.12	0.067	8.60	0.055
M36859Q	C12	-1	0.12	0.053	7.89	0.028
M36860T	C13	1	0.10	0.060	7.94	0.149
M36861F	C14	-1	0.11	0.050	7.19	0.030
M36862S	C15	0	0.12	0.046	7.87	0.028
M36863F	C16	-1	0.08	0.050	6.41	0.015
M36864R	C17	0	0.11	0.055	8.96	0.020
M36865E	C18	-1	0.11	0.049	8.63	0.017
M36866R	C21	0	0.13	0.050	9.17	0.020
M36867D	C31	0	0.15	0.056	9.27	0.021
M36868Q	P11	106	0.21	0.052	9.87	0.054
M36869D	P12	113	0.22	0.055	9.01	0.051
M36870F	P13	107	0.24	0.052	8.58	0.037
M36871B	P14	110	0.23	0.059	9.16	0.101
M36872W	P15	108	0.26	0.052	9.29	0.034
M36873R	P16	113	0.23	0.052	9.17	0.037
M36874N	P17	107	0.28	0.051	9.29	0.030
M36875I	P18	111	0.24	0.058	10.67	0.031

Table B3: ICP results on samples of different time(contd.)

Name		Co	Ni	Cu	Zn	As
M36858M	C11	0.01	3.90	19.348	12.083	0.073
M36859Q	C12	0.01	3.76	15.430	12.189	0.081
M36860T	C13	0.01	3.75	19.967	12.154	0.081
M36861F	C14	0.01	3.80	15.591	12.126	0.087
M36862S	C15	0.00	3.93	15.421	12.463	0.081
M36863F	C16	0.01	3.83	14.009	12.513	0.070
M36864R	C17	0.01	4.18	14.859	13.293	0.093
M36865E	C18	0.01	4.05	15.032	13.065	0.087
M36866R	C21	0.00	4.21	14.712	13.163	0.085
M36867D	C31	0.01	4.24	15.265	13.693	0.084
M36868Q	P11	0.00	4.13	17.003	13.282	0.106
M36869D	P12	0.007	4.450	18.650	14.596	0.102
M36870F	P13	0.01	4.31	17.015	14.093	0.118
M36871B	P14	0.01	4.42	20.558	14.511	0.115
M36872W	P15	0.01	4.51	16.908	14.349	0.118
M36873R	P16	0.01	4.65	17.429	14.436	0.132
M36874N	P17	0.008	4.445	16.500	14.508	0.116
M36875I	P18	0.013	4.749	16.633	14.529	0.111

Table B3: ICP results on samples of different time(contd.)

Name		Pd	Ag	Pt	Au	Pb
M36858M	C11	17.389	0.524	30.274	20.894	13.212
M36859Q	C12	17.857	0.430	30.627	20.353	12.975
M36860T	C13	17.620	0.609	30.458	13.897	13.022
M36861F	C14	15.534	0.167	32.250	10.371	13.192
M36862S	C15	15.418	0.203	32.693	0.111	13.429
M36863F	C16	15.320	0.080	32.843	0.025	13.238
M36864R	C17	15.597	0.080	31.697	0.022	13.190
M36865E	C18	15.226	0.068	32.393	0.018	13.356
M36866R	C21	14.721	0.055	31.682	0.017	8.138
M36867D	C31	15.049	0.080	32.361	0.016	7.640
M36868Q	P11	15.327	0.551	31.937	17.465	12.726
M36869D	P12	15.663	0.512	31.187	16.626	12.235
M36870F	P13	15.522	0.457	30.599	11.365	11.007
M36871B	P14	15.625	0.366	30.257	0.300	10.541
M36872W	P15	15.615	0.165	29.728	0.058	9.805
M36873R	P16	15.858	0.158	29.622	0.034	9.684
M36874N	P17	15.736	0.137	29.497	0.020	9.706
M36875I	P18	15.606	0.102	29.328	0.032	9.152

Table B4: ICP results on samples of different solid/liquid ratio

Name		Ca	Ti	V	Cr	Fe
M36866R	C21	0	0.13	0.312	0.050	9.17
M36867D	C31	0	0.15	0.305	0.056	9.27
M36876D	P21	249	0.24	0.283	0.055	8.65
M36877Z	P31	264	0.25	0.268	0.055	7.27

Name		Co	Ni	Cu	Zn	As
M36866R	C21	0.00	4.21	14.712	13.163	0.085
M36867D	C31	0.01	4.24	15.265	13.693	0.084
M36876D	P21	0.039	92.968	16.451	14.621	0.120
M36877Z	P31	0.006	4.445	15.631	13.680	0.120

Name		Mo	Pd	Ag	Pt	Au
M36866R	C21	-0.001	14.721	0.055	31.682	0.017
M36867D	C31	0.006	15.049	0.080	32.361	0.016
M36876D	P21	0.015	14.636	0.074	28.992	0.016
M36877Z	P31	0.006	16.194	0.052	30.177	0.020

Table B5: ICP results on samples of different time at different solid liquid ratio

Name		Cr	Fe	Mn	Co
		ppm	ppm	ppm	ppm
Limit of Detection		0.000	0.00	0.000	0.00
BLANK-OM		0.002	0.04	0.000	0.00
AU -100PPB		0.002	0.04	0.000	0.00
AU-1PPM		0.005	0.19	0.002	0.00
M37235P	C1	0.428	17.78	0.098	0.06
M37255O	P1	2.857	129.09	0.540	0.09
M37236U	C2	2.445	103.01	0.857	0.22
M37256A	P2	1.591	57.79	0.439	0.14
M37237Y	C3	2.200	71.87	0.326	0.17
M37257M	P3	2.391	7.38	0.061	0.07
M37221B	C11	0.269	0.45	0.052	-0.01
M37222B	C12	0.363	2.63	0.081	0.03

M37223C	C13	1.642	9.81	0.291	0.03
M37224D	C14	1.811	4.79	0.110	-0.12
M37225D	C15	7.799	14.63	1.299	-0.06
M37226E	C16	2.131	2.54	0.304	-0.09
M37227E	C17	1.967	0.67	0.403	-0.10
M37228F	C21	0.096	-5.20	0.044	-0.03
M37229F	C22	0.202	-11.82	0.060	-0.03
M37230T	C23	0.109	-18.83	0.098	0.00
M37231Y	C24	0.072	-5.11	0.021	-0.01
M37232C	C25	0.064	-18.86	0.043	-0.01

Table B5: ICP results on samples of different time at different solid liquid ratio (contd.)

Name		Cr	Fe	Mn	Co
		ppm	ppm	ppm	ppm
M37233G	C26	0.065	-19.02	0.013	-0.03
M37234L	C27	0.064	4.02	0.038	0.01
M37241U	P11	0.061	-6.08	0.038	-0.02
M37242D	P12	0.101	-1.48	0.063	-0.02
M37243L	P13	0.068	-1.24	0.072	-0.01
M37244T	P14	0.221	-1.27	0.030	0.02
M37245C	P15	-0.661	-11.70	0.263	0.04
M37246K	P16	0.283	-3.44	2.633	0.01
M37247S	P17	0.229	-0.65	0.399	-0.03
M37248A	P21	0.163	-4.20	0.302	-0.03
M37249J	P22	1.589	-9.05	0.836	-0.33
M37250P	P23	0.086	0.47	0.057	-0.026
M37251R	P24	0.064	-0.38	0.091	-0.03

M37252D	P25	-0.054	3.88	0.116	0.00
M37253P	P26	0.135	7.23	0.048	-0.03
M37254C	P27	-0.852	-49.98	0.249	-0.26
M37238D	C4	-0.200	-40.54	0.278	-0.05
M37258Y	P4	-1.645	-60.90	0.139	-0.04
M37239H	C5	-1.950	-113.46	0.125	-0.14
M37259K	P5	0.083	4.84	0.034	-0.023
M37240M	C6	0.152	6.10	0.057	-0.023
M37260Y	P6	0.037	3.48	0.615	-0.045

Table B5: ICP results on samples of different time at different solid liquid ratio (contd.)

Name		Ni ppm	Cu ppm	Zn ppm	Au ppm
Limit of Detection		0.00	0.0	0.000	0.000
BLANK-OM		0.00	0.0	0.004	0.003
AU -100PPB		0.00	0.0	0.024	0.068
AU-1PPM		0.01	0.0	0.009	0.591
M37235P	C1	0.94	0.4	1.724	4.1
M37255O	P1	6.58	1.9	5.436	1.6
M37236U	C2	9.23	9.3	22.626	0.4
M37256A	P2	7.04	1.0	1.608	63.1
M37237Y	C3	6.90	2.3	5.927	40.9
M37257M	P3	2.82	1.5	2.587	393.3
M37221B	C11	0.51	0.3	0.799	68.8
M37222B	C12	1.25	0.6	1.165	20.6
M37223C	C13	4.97	1.5	1.536	24.7
M37224D	C14	5.80	0.4	0.168	11.9
M37225D	C15	7.64	24.9	3.903	25.3
M37226E	C16	9.22	0.9	0.799	12.4
M37227E	C17	10.72	0.1	3.846	6.1
M37228F	C21	-0.01	0.3	0.535	59.6

M37229F	C22	0.51	0.0	0.823	25.9
M37230T	C23	0.45	0.3	3.707	9.2
M37231Y	C24	0.44	0.249	0.730	6.8
M37232C	C25	0.54	0.134	0.361	14.9
M37233G	C26	0.45	0.124	0.070	18.6
M37234L	C27	0.40	0.744	0.804	9.1
M37241U	P11	0.40	0.773	1.915	0.9
M37242D	P12	-0.58	0.031	0.093	12.6
M37243L	P13	0.63	2.621	3.641	5.6
M37244T	P14	-0.26	0.762	0.758	9.6
M37245C	P15	0.16	-0.302	0.534	2.9
M37246K	P16	1.27	0.595	4.161	14.5
M37247S	P17	1.25	4.293	12.195	3.3
M37248A	P21	-3.37	-0.386	4.143	10.8
M37249J	P22	-1.98	2.249	5.313	4.6
M37250P	P23	-0.465	-0.009	0.403	3.1
M37251R	P24	-0.94	0.095	0.750	7.2
M37252D	P25	2.52	0.285	0.767	5.2
M37253P	P26	-1.28	0.429	1.100	7.1
M37254C	P27	-4.84	0.1	-0.475	1.1
M37238D	C4	8.08	20.9	62.901	377.0
M37258Y	P4	5.65	5.7	4.147	22.6

M37239H	C5	9.40	0.4	3.570	343.5
M37259K	P5	0.316	1.132	1.175	76.6
M37240M	C6	0.760	2.953	4.496	436.6
M37260Y	P6	1.075	-0.035	0.969	8.2



